Tsukasa Seya
Misako Matsumoto
Takashi Ebihara
Hiroyuki Oshiumi

Functional evolution of the TICAM-1 pathway for extrinsic RNA sensing

Authors' address
Tsukasa Seya[1], Misako Matsumoto[1], Takashi Ebihara[1], Hiroyuki Oshiumi[1]
[1]Department of Microbiology and Immunology, Hokkaido University Graduate School of Medicine, Sapporo, Japan.

Correspondence to:
Tsukasa Seya
Department of Microbiology and Immunology
Hokkaido University Graduate School of Medicine
Kita 15, Nishi 7, Kita-ku
Sapporo 060-8638
Japan
Tel.: +81 11 706 5073
Fax: +81 11 706 7866
e-mail: seya-tu@pop.med.hokudai.ac.jp

Acknowledgements
We thank Drs A. Matsuo, T. Tsujita, A. Ishii, M. Shingai, M. Sasai, and K. Funami in our laboratory for their valuable discussions. This work was supported in part by CREST, JST (Japan Science and Technology Corporation), and by Grants-in-Aid from the Ministry of Education, Science, and Culture (Specified Project for Advanced Research) and the Ministry of Health, Labor, and Welfare of Japan, and by the Takeda Science Foundation, Uehara memorial Foundation, Northtec Foundation, Akiyama Foundation and Mitsubishi Foundation. Financial supports by the Sapporo Biocluster 'Bio-S' the Knowledge Cluster Initiative of the MEXT, and the Program of Founding Research Centers for Emerging and Reemerging Infectious Diseases, MEXT are gratefully acknowledged.

Immunological Reviews 2009
Vol. 227: 44–53

Immunological Reviews
0105-2896

Summary: The type I interferon (IFN) is a host defense factor against microbial pathogens in vertebrates. In mammals, retinoic acid-inducible gene I (RIG-I) and melanoma differentiation-associated gene 5 (MDA5) in the cytoplasm are regarded as sensors for double-stranded RNA (dsRNA) and trigger IFN regulatory factor-3 (IRF-3) activation followed by type I IFN induction through the mitochondrial antiviral signaling (MAVS) adapter. This intrinsic pathway appears to link the main protective responses against RNA virus infection in mammals. On the other hand, human Toll-like receptor 3 (TLR3) is localized in the endosomal membrane or cell surface and signals the presence of extrinsic dsRNA. In response to RNA stimulation, TLR3 recruits the Toll-interleukin 1 receptor domain (TIR)-containing adapter molecule 1 (TICAM-1) adapter and induces IRF-3 activation followed by IFN-β promoter activation. Human TLR3 is localized limitedly extent in myeloid dendritic cells, fibroblasts, and epithelial cells. The TICAM-1 and cytoplasmic MAVS pathways converge at the IRF-3-activating kinase in human cells. The reason for the involvement of this extrinsic mode of IFN-inducing pathways in the dsRNA response remains unknown. In fish, two TLRs, i.e. endoplasmic TLR3 and cell surface TLR22, participate in teleost IFN production without the activation of IRF-3. TLR22 is distinct from mammalian TLR3 in terms of cellular localization, ligand selection, and tissue distribution. TLR22 may be a functional substitute for human cell surface TLR3 and may serve as a surveillance molecule for detecting dsRNA virus infection and alerting the immune system for antiviral protection in fish. In this review, we discuss the fundamentals of the extrinsic dsRNA recognition system, which has evolved to induce cellular effectors to cope with dsRNA virus infection across different vertebrate species.

Keywords: *Toll-like receptor, evolution, dsRNA recognition, TICAM-1 (TRIF)*

Introduction

Invading pathogens express specific pattern molecules and are recognized by host pattern recognition receptors (PRRs) (1, 2), representatives of which are Toll-like receptors (TLRs), Nod-like receptors (NLRs), and RNA helicases [retinoic acid-inducible gene I (RIG-I), melanoma differentiation-associated protein 5 (MDA5), etc.]. These receptors signal the presence of microbial patterns in myeloid dendritic cells (mDCs) and thus induce potent activation of the systemic host defense response (3). Recent studies on pattern receptors of

the innate immune system have increased our understanding of how mDCs mature through infection and subsequently orchestrate cellular immunity (4, 5). These molecules also serve as adjuvants for the induction of antigen-specific acquired immunity. TLRs, RIG-I-like helicases (RLHs), and NLRs are major targets for investigating the induction of robust acquired immune responses upon pathogen stimulation. These studies have been conducted using gene-disrupted mice and in *in vitro* human systems.

It has been reported that human cells induce interferon-β (IFN-β) in response to various RNA structures (6, 7). Double-stranded RNA (dsRNA) and its analog polyinosinic–polycytidylic acid (polyI:C) have been identified as potent immune stimulators of viral patterns and are recognized by PRRs. PRRs link cytoplasmic adapter molecules in these mammalian cells. Cytoplasmic RLH and membrane-associated TLRs that induce IFN-α/β involve the mitochondrial antiviral signaling (MAVS) (also known as IPS-1, Cardif, or VISA) or TICAM-1 [Toll-interleukin-1 receptor (IL-1R) (TIR) domain-containing adapter-inducing IFN-β (TRIF)] adapters, respectively, to converge the signal at IRF-3-activating kinases for IFN-β induction (4, 5, 8). IFN-β induction is IRF-3 dependent in mDCs and fibroblasts/epithelial cells (4, 5). By contrast, IFN-α/β is differentially induced in an IRF-7-dependent manner in plasmacytoid DCs (pDCs) (9). This allows activation of the myeloid differentiation factor 88 (MyD88) adapter protein and IKKα [inhibitor of nuclear factor (NF) κB (IκB) kinase α] kinase, which directly activates the IRF-7 transcription factor (10). However, the molecular assembly and mechanism involved in polyI:C-mediated activation of transcription factors still remain unclear in mice and humans.

Some PRRs preferentially recognize nucleic acid structures that are unique to infectious microbes. Type I IFN induction and cytotoxic T-lymphocyte (CTL)/natural killer (NK) cell activation are major outputs for RNA-sensing PRRs in mammalian cells (5, 11). A variety of RNA sensors in the cytoplasm or membranes are engaged in the detection of microbial RNA. These are expressed in a cell-type specific fashion and participate in IFN-α/β production in various cell types. However, the combinations of these receptors that induce cellular immunity still remain undetermined. It is generally accepted that RNA patterns that are exogenously provided or are produced in bystander cells are internalized by mDCs through phagocytosis and are then recognized by endosomal PRRs. By contrast, RNA patterns produced in the cytoplasm of infected cells are directly recognized by PRRs present in the cytoplasm (12). In this review, we adopted an evolutional approach to study TLRs present on the cell membrane and the recognition of the external dsRNA pattern that is specifically formed in other cells during virus replication.

Fish (teleost) have >20 TLRs that include orthologs of human TLRs and other TLRs unique to lower vertebrates living in water (13, 14). Teleost have orthologs of the IFN-inducing genes of mammals and PRRs for microbial pattern recognition. Teleost also have a TICAM-1 ortholog which has no TRAF-binding site but retains the RIP1-binding site (15, 16). Fish may have orthologs of RLH and NLRs. Hence, by comparing the mammalian PRR receptor/adapter system with that of fish, it is possible to examine the development of the innate recognition system during evolution. Molecular evolution by which the mammalian immune system has been established in the current form can be analyzed through the genomic information of vertebrate TLR systems. In this study, we cast insight into the functional properties of fish TLRs and adapters involved in IFN induction.

Recognition of RNA duplexes in vertebrates

Viral replication usually generates dsRNA in the cytoplasm of infected cells and signals to activate antiviral responses. dsRNA, stem-loop structure of RNA, 5′-uncapped triphosphate of RNA, and specific RNA sequences are rapidly recognized by PRRs in the cytoplasm (4, 5, 17), then implicated in host defense (Fig. 1). Many pattern-sensing receptors have been identified in mammals: PKR (dsRNA-dependent protein kinase), Dicer of the short interfering/microRNA system, RLHs including RIG-I, MDA5, and LGP2, and other helicases. These receptors are accompanied by adapters that transduce the dsRNA-sensing signal downstream. Other RNA-sensing molecules such as helicases may also be present in the cytoplasm to join a molecular assembly for foreign RNA detection. The synthesized dsRNAs are incorporated into these molecular complexes to prohibit RNA replication in virus-infected cells.

TLR3 is present in the early endosome and can recognize dsRNA delivered inside the endosomal membrane (18). TLR3 may not have a direct role in capturing dsRNA generated by virus replication in the cytoplasm, but it has an important role in trapping phagocytosed dsRNA (Fig. 2), which is usually wrapped in a membrane that originates from the infected cell (19). In comparison to the direct recognition system of dsRNA in the cytoplasm, this mode of RNA recognition is unique and sophisticated, concerning activation of cellular immunity. As RNA-sensing TLRs and RLH are conserved across vertebrates (20), we hypothesize

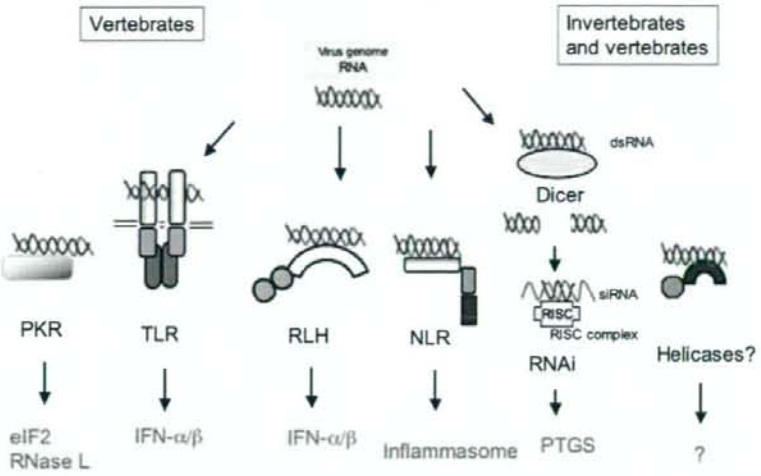

Fig. 1. Various RNA sensors in vertebrates. dsRNA are generated during virus replication. Major RNA sensors in vertebrate cells and their responses on stimulation with dsRNA are indicated. Dicer and RNA-recognizing helicases work even in invertebrates. How dsRNA selects a variety of RNA pattern sensors remains largely unknown. PTGS, post-transcriptional gene silencing.

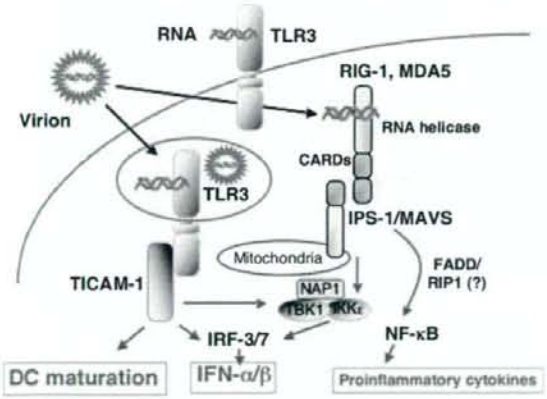

Fig. 2. Cell surface, endosomal and cytoplasmic recognition of dsRNA in mammalian cells. TLR3 is distributed either on the cell surface or in the endosome. Its distribution ratio depends on cell types. RLH (RIG-I and MDA5) reside in the cytoplasm. Adapter molecules, TICAM-1 and MAVS, are localized in the cytoplasm. Upon stimulation, TLR3 recruits TICAM-1 near the endosomal membrane, while MAVS recruits RLH on the mitochondrial membrane. The known outputs of TLR3 and RLH are indicated by red. TLR, Toll-like receptor; RIG, retinoic acid-inducible gene; RLH, RIG-I-like helicase; TICAM, Toll-interleukin 1 receptor domain-containing adapter molecule.

that the two distinct pathways of dsRNA recognition were established in a vertebrate ancestor ~500 Ma and that the two systems have been preserved in mammals (Fig. 2). We focus on the fish membrane-associated dsRNA recognition system and analyze it in terms of its physiological significance and functional feature and also from an evolutionary point of view. We also address the question of why vertebrates need the surface system for dsRNA recognition in addition to the cytoplasmic virus-sensing systems.

Surface recognition of dsRNA in mammals

We initiated a study on the functions of the membrane-associated dsRNA recognition receptor TLR3 in human cells. Stimulation of human fibroblasts/epithelial cells with polyI:C leads to the production of type I IFN. We have produced monoclonal antibodies (mAbs) against human TLR3 and obtained one which blocks polyI:C binding to TLR3, named the mAb TLR3.7 (21). The TLR3.7 mAb interferes with IFN-β production induced by exogenously added polyI:C in human fibroblasts/epithelial cells (18, 21). Hence, it appears that TLR3.7 mAb blocks the interaction between TLR3 and polyI:C on the cell surface by binding to TLR3. If this is the case, human TLR3 must be localized on the cell surface of the fibroblast to capture external dsRNA. This hypothesis was proven by results from fluorescence-assisted cell sorting (FACS) and imaging analyses (Fig. 3A). However, using the same mAb, human mDC TLR3 could not be detected on the surface (18) but was found to be localized in intracellular compartments, particularly endosome (Fig. 3A). mDCs respond to polyI:C to induce type I IFN in the early endosome (22, 23). In this case, how does endosomal TLR3 recognize polyI:C outside the cells? It is rational that there is a transporter that shuttles dsRNA from the cell surface to the endosome in mammals (5). The recognition of dsRNA by TLR3 on the cell surface is

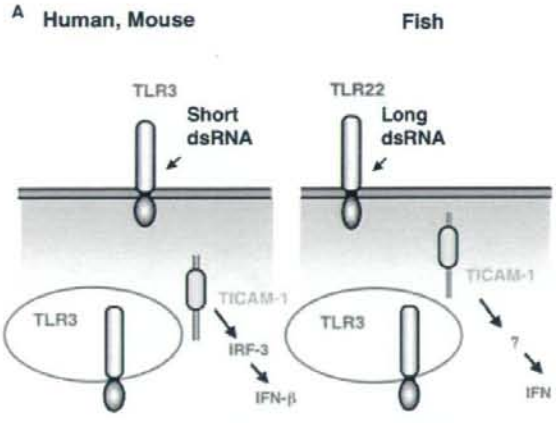

B **IFN-inducing receptors in human and fish**

Genes	Human	Fish
TLR3	+	+
RIG-I	+	–
TLR22	–	+
IFN	+	+

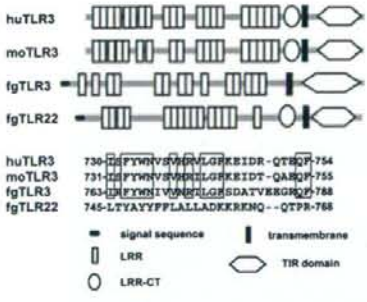

Fig. 3. Different TLRs cover surface dsRNA recognition in fish and mammals. (A) TLR3 and TLR22 in vertebrates. In human and mouse, TLR3 encompasses cell surface and endosomal RNA sensing and induces IRF-3 activation. In fish, two distinct gene products, TLR3 and TLR22, participate in dsRNA sensing. IFN is induced in an IRF-3-independent fashion. Although the structural information is not shown in the panel, mammalian TICAM-1 structurally differs from fish TICAM-1. IRF-3-activating kinase indirectly assembles in an N-terminal portion of mammalian TICAM-1 but not fish TICAM-1. A C-terminal portion contributes to IFN promoter activation in fish cells. (B). Difference of IFN-inducing receptors between human and fish. Upper table indicates that humans lack TLR22 while fish lack RIG-I, although both have IFN-inducible pathways. The structural differences among human (hu) TLR3, mouse (mo) TLR3, fgTLR3, and fgTLR22 are depicted in the lower panel. The primary structures of the linker region (a determinant of TLR3 localization) are shown below the structural models.

experimentally proven by using the mAb probe for determining the localization of human TLR3. However, the dsRNA shuttling system has not yet been proved.

If TLR3 participates in the induction of IFN-β in epithelial cells, its downstream molecules should activate IRF-3. Therefore, we searched for an adapter molecule that could directly interact with TLR3 and activate IRF-3; the molecule was identified by employing the yeast two-hybrid system. It was named TICAM-1 (24) and is now popularly known as TRIF (25).

Human TICAM-1 consists of an N-terminal region (1–234), a TIR domain (235–500), and a C-terminal region (501–680). The N-terminal region of TICAM-1 harbors tumor necrosis factor (TNF) receptor-associated factor (TRAF) family proteins (26, 27) and forms a complex containing IRF-3-activating kinases (28, 29). This kinase complex is crucial for activating the IFN-β promoter (28, 29) and inducing the activation of NK (5, 30) and CTL (12, 31) effector cells (Fig. 4). The C-terminal region of TICAM-1 can recruit receptor-interacting protein-1 (RIP-1), and this event is followed by the activation of other effectors (32). All these signaling events constitute the TICAM-1 pathway. Human and mouse TICAM-1 pathways involve mDC maturation, cytokine/chemokine induction, cross-presentation of exogenous antigens for proliferation of $CD8^+$ T cells (5, 12, 31, 33), NK cell activation (30, 34), and induction of autophagy and apoptosis (35). CD4+ regulatory T (Treg) cells and Th17 cells may be induced by mDCs matured through TICAM-1 signaling. TICAM-1 may act as a platform that recruits various signaling molecules for mDC output in mammals. However, one question that remains unanswered is whether the TICAM-1 pathway is conserved in lower vertebrates such as fish.

Surface recognition of dsRNA in fish

Fish [*Takifugu rubripes* (fg)] have ~20 TLRs and three TLR adapters, i.e. fgMyD88, fgTICAM-1, and fgTIRAP/Mal (36). By using the yeast two-hybrid analysis system, we found at least two TLRs that share the fgTICAM-1 adapter (37). The first report on fgTLRs (13) showed that fgTLR3 and fgTLR22 choose the fgTICAM-1 adapter in fish cells and induce fish type I IFN by recognizing dsRNA. fgTLR3 and fgTLR22 are quite different in their primary structures (Fig. 3B) and are classified into different clades by gene tree analysis (13, 37). However, both fgTLR3 and fgTLR22 directly bind to fgTICAM-1 in fish cells as well as in yeast. Confocal analysis has shown that fgTLR3 resides in the endoplasmic reticulum (ER) and recognizes relatively short dsRNA, whereas fgTLR22 recognizes long dsRNA present on the cell surface (37). The

properties of fgTLR3 and fgTLR22 are summarized in Fig. 3B. fgTLR22 is particular, as fgTLR22 preferentially recognizes long dsRNA, localizes exclusively to the cell surface, and is widely distributed across tissue/organs. In summary, two of the receptors that recognize dsRNA are also involved in the TICAM-1 pathway in fish. The fish TICAM-1 pathway leads to the activation of the IFN promoter.

The next question is how TICAM-1 is assembled by TLR22 to transmit the dsRNA recognition signal. Possible answers may lie in the structural difference between mammalian and teleost TICAM-1 (Fig. 3B). Over-expression of zebrafish (zf)TICAM-1 activates the zfIFN promoter, but zfTICAM-1 does not interact with zfTRAF6 (16). Results from genomic retrieval analysis suggest that zebrafish lacks IRF-3. The zfTICAM-1 N-terminal region does not contain the TRAF6-binding motif (that participates in IRF-3 activation), and the C-terminal region of zfTICAM-1 can adequately activate the zfIFN promoter. This observation suggests the involvement of RIP1-mediated NF-κB activation in zfIFN promoter activation (16, 37).

Human TICAM-1 stimulates IRF-3-mediated type I IFN induction by means of its N-terminal region (38, 39) (Fig. 4). Thus, fish TICAM-1 behaves like human TICAM-1; however, fish TICAM-1 does not employ IRF-3 to activate the IFN-β promoter (16, 40). Although the TICAM-1 pathway is conserved across both fish and humans, the molecular bases for IFN induction in response to extrinsic dsRNA differ in the two vertebrate species (Fig. 3). Our speculation is that although fish cells have an IFN output similar to that of human cells, the signal cascade that leads to IFN production is modally different. Teleost TICAM-1, which is structurally dissimilar to human TICAM-1 (36), might help in explaining the differential selection of the signal pathways.

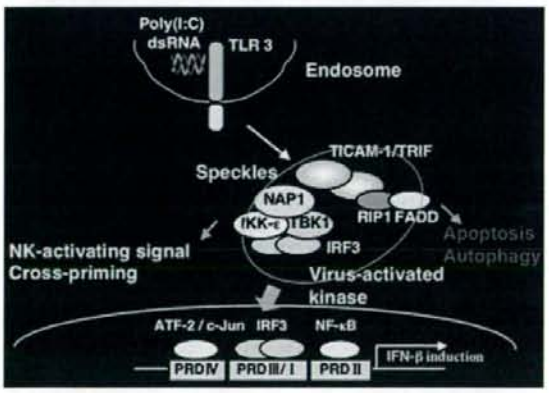

Fig. 4. TICAM-1 is dissociated from TLR3 to form a signaling unit, Speckle. In human cells, TICAM-1 once detached from TLR3 serves as a signaling platform to induce apoptosis, autophagy, NK activation, and cross-priming. TICAM-1 undergoes some modification secondary to complex formation with TLR3 and dissociated from TLR3 with unknown mechanism. The pathways for NK activation, CTL induction, and autophagy are not yet identified, although the pathway for apoptosis is getting clarified. It is undetermined whether surface-expressed TLR3 or TLR22 retain the cellular responses.

How does human TLR3 substitute for TLR22 in mammals?

The differences between TLR22 and TLR3 can be summarized as follows. Based on confocal microscopy and FACS analyses, over-expressed fgTLR22 is localized on the cell surface, while fgTLR3 resides in the ER and endosomes in fish cells (37). fgTLR22 is ubiquitously distributed over the organs/tissues of teleost, while human and fgTLR3 are present only in a limited cell repertoire. These two TLRs do not merge with each other or with fgTICAM-1 in resting cells. When stimulated with polyI:C, a part of the fgTLR22 population enters the cytoplasmic region to merge with fgTICAM-1 (37). Similarly upon stimulation, fgTLR3 is clustered and merges with fgTICAM-1 in the cytoplasm (37). Immunoprecipitation studies have supported their molecular interactions: fgTICAM-1 coprecipitates with fgTLR22 or fgTLR3 in human HEK293 cells. A reporter assay has shown that the dominant-negative form of fgTICAM-1 blocks the fgTLR22- and fgTLR3-mediated IFN promoter activation induced by endogenous fgTICAM-1 in RTG-2 (rainbow trout) cells. Thus, fish have a novel TICAM-1-coupling TLR, TLR22, which is clustered on the cell surface. Although mammals have lost TLR22, TLR3 is distributed on the surface membrane as well as in the endosomes only in some kinds of epithelial cells (41–44), and this appears as though TLR3 compensates for the loss of TLR22 in limited cell types.

We tested the physiological function of fgTLR22 and found that fgTLR22-expressing RTG-2 (rainbow trout) cells become resistant to virus infection (37). We used birnavirus, which is a representative dsRNA virus found in water. Cytopathic effect formation was observed in control cells that did not express fgTLR22, whereas it was barely detected in cells expressing fgTLR22. The level of TCID50 in the supernatant, which reflects virus replication in the cells, was high in the control cells and ~100-fold lower in fgTLR22-expressing cells. Virus RNA levels were suppressed in fgTLR22-expressing cells. Conversely, IFN mRNA was upregulated in virus-infected cells.

In humans, TLR3 is expressed in the endosomes and on the surface of epithelial cells/fibroblasts (18, 22). Expression of TLR3 on the cell surface membrane of human bronchial, bile-duct, and intestinal epithelial cells has also been reported

(41–44). Thus, surface-expressed human TLR3 appears to be a functional remnant of fish TLR22: TLR3 functions in the mucosal region wherein body fluids are continuously in contact with the flora. Because cell surface-associated dsRNA recognition is indispensable even in humans, TLR3 is expressed on human fibroblasts and epithelial cells. Likewise, TLR22 may be a functional substitute for human cell surface TLR3 and may act as a surveillance molecule for detecting dsRNA virus infection.

Evolution of the surface RNA recognition system in vertebrates

The results from bootstrap probability analysis indicate that TLR22 does not belong to the TLR3 family and is instead proximal to mouse TLR13, which has not been characterized as a dsRNA-recognizing TLR. Thus, two arms of the TICAM-1 pathway have evolved as dsRNA receptors in fish, and only TLR3 has been preserved in mammals (*Table* 1). Development of TLR22 instead of TLR3 may afford some advantage for protection against RNA viruses by augmenting the susceptibility of the local IFN response to long RNA duplexes.

We wanted to understand why teleosts require a cell surface RNA recognition system. Fish live in water and are exposed to many kinds of negative-stranded RNA viruses belonging to the Rhabdoviridae and dsRNA viruses (45, 46). Bacteria such as *Rhodovulum sulfidophilum* and perhaps other species are involved in the extracellular liberation of ribosomal and transfer RNAs into the sea (47). Thus, the sea may contain RNA viruses and RNA products of microbial origin. The sea is home to a unique and mysterious microbial environment. During evolution, vertebrates in water may have been protected from these pathogens by developing a set of RNA-sensing TLRs and an IFN system, which are distinct from those expressed in land animals. Our studies indicate that RNA sensing by TLRs protects fish from spreading or exacerbating infection. Land animals preserve the surface RNA recognition system to a limited extent in their epithelial ducts where the microbial environment is retained similar to that found in the sea.

Over-expressed teleost TLR22 protects host cells from infection with IPNV, which is a naked bisegmented dsRNA virus belonging to the family Birnaviridae (48). Birnaviruses have a single $T = 13$ *icosahedral* shell that is composed of 120 subunits, and these viruses lack the characteristic inner capsid. Aquatic birnaviruses are distributed worldwide, can infect a range of fish and shellfish species (45, 46), and are viral pathogens that cause diseases in fry and young fish. Although teleosts have the gene that encodes a putative ortholog of the cytoplasmic RNA sensor MDA5 (36, 49), IPNV efficiently infects teleost cells unless TLR22 is expressed in some population of cells. Thus, fish MDA5 is insufficient for protection against this type of dsRNA virus. Although all cells do not express TLR22, IFN seems to be sufficiently induced by TLR22-expressing cells to provide an antiviral environment in surrounding cells, resulting in host cell protection. However, the manner in which TLR22 detects the IPNV infection remains to be clarified. The necessity of TLR22 and its mode of dsRNA recognition in fish are of interest for further investigation.

Effector induction by endosomal TLR3 in mammals

We produced a TICAM-1 knockout (KO) mouse and tested the effector-inducing properties using the syngeneic tumor implant system of this mouse (30, 50). PolyI:C was intraperitoneally administered as the ligand for TLR3 stimulation. In this system, RLH may sense polyI:C similarly in TICAM-1 KO as well as in wildtype mice, but detectable phenotypes shouldreflect only the difference in TICAM-1 in mice. Mouse melanoma line B16

Table 1. Repertoire of pattern recognition receptors in vertebrates

	TLR																			
	1	2	3*	4	5	6	7	8	9	10	12	13	14	21	22*	MyD88	TICAM*	RIG-I	MDA-5	IPS-1	IFN
Human	+	+	+	+	+	+	+	+	+	+	–	–	–	–	–	+	+	+	+	+	+
Mouse	+	+	+	+	+	+	+	+	+	*psd*	+[†]	+	–	–	–	+	+	+	+	+	+
Chicken	+	+	+	+	+	*psd*	+	–	–	–	–	–	+[‡]	+	–	+	+	–	+	*frg*	+
Xenopus	+	+	+	+	+	±	+	+	+	±	+	+	+	+	+	+	+	+	+	*frg*	+
Fugu	+	+	+	–	+	–	+	+	+	–	–	–	+	+	+	+	+	–	+	*frg*	+
Zebra	+	+	+	+	*frg*	–	*frg*	*frg*	+	–	+	–	+	*frg*	+	+	+	–	+	*frg*	+
Ascidia	~3?															–	–	–	–	–	–
Sea urchin	~300?															7	2	6?	6?	1?	–

psd, pseudogene; *frg*, fragment.
*TLR3, TLR22, and TICAM are IFN-inducing genes.
[†]Mouse TLR11.
[‡]Bird TLR15.
Ascidia and Sea urchin are invertebrate references.

[low major histocompatibility complex (MHC) expresser] and the C57BL/6 cell lines were used in this study.

The tumors grew well in wildtype mice. When polyI:C was administered intraperitoneally, tumor growth was retarded. Similar results were obtained with MyD88 KO, PKR KO, and IFN-β KO mice. PolyI:C-mediated tumor growth retardation was completely abrogated in TICAM-1 KO mice, suggesting that TICAM-1 is crucial for tumor-directed effector induction. IFN-β is an output of the activation of the TICAM-1 pathway, but it barely affects tumor regression. Retardation of tumor growth by polyI:C was completely abrogated in wildtype mice by depletion of NK1.1- or asialoGM-1-positive cells (30). Tumor growth suppression in response to polyI:C was normally observed in $CD8^+$ T-cell-depleted mice. Hence, NK/NKT cells, not CTLs, are effectors responsible for tumor regression in this mouse model with low MHC-expressing tumor. As polyI:C activates the TICAM-1 pathway, size reduction of the implant tumor reflects the potential of the effectors induced by the functioning of the TICAM-1 pathway (Fig. 5).

We next checked whether TICAM-1 in mDCs or other immune cells is important for tumor growth retardation. TICAM-1 was transfected into bone marrow-derived DCs (BMDCs), and these cells were adoptively transferred to mice with tumor burden. Tumor growth was significantly reduced in mice injected with TICAM-1-positive BMDCs but not in those injected with other BMDCs that did not express TICAM-1 (50). Thus, the mDC TICAM-1 pathway is involved in anti-tumor NK activation (30) (Fig. 5).

The TICAM-1 pathway activates transcription factors, IFN regulatory factor-3 (IRF-3), IRF-7, activator protein 1 (AP1), and NF-κB in mouse cells. The results from our in vitro NK assay suggest that IRF-3 largely participates in mDC-NK reciprocal activation (T. Ebihara, M. Matsumoto, T. Seya, unpublished data). Actually, polyI:C-mediated tumor growth retardation was abrogated in IRF-3 KO mice but not IRF-7 KO mice. Thus, in mDCs, induction of the molecules that drive NK activation would depend on IRF-3 activation.

We found that tumor-specific CTLs are induced by polyI:C when EG7 cells [a high MHC expresser with ovalbumin (OVA)] are employed as the implant tumor. Therefore, we checked the levels of the OVA epitope-responsive $CD8^+$ T cells, i.e. OT-1. BMDCs expressing TICAM-1 potentially induce T-cell proliferation and IFN-γ induction (Fig. 4). These T-cell responses are largely independent of IRF-3 or IRF-7 in mDCs (M. Azuma, T. Ebihara, M. Matsumoto, T. Seya, unpublished data). Thus, when implant tumor expresses high levels of MHC, CTLs driven through mDCs act as the main effector cell in mice (31). CTLs and NK cells are induced by distinct routes in mDCs (51, 52).

Cellular immune activation by mDCs depends on the situation of TLR3-adapter complex. Cytoplasmic activation of the

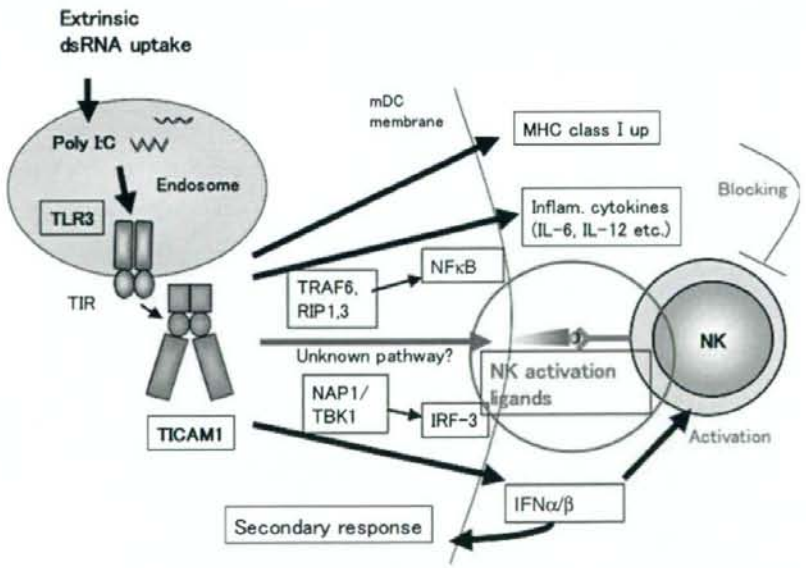

Fig. 5. Mechanism of mDC-NK reciprocal activation induced by dsRNA stimulation of mDCs. TICAM-1 has a crucial role in NK activation driven by polyI:C-stimulated mDCs in human cells. When TLR3 grasps the dsRNA signature in the endosome of mDCs, TICAM-1 in mDCs is activated to evoke a signal pathway reaching to the expression of NK-activating ligands. NK cell activation is then induced via mDC-NK contact. Some soluble factors may be important for NK activation in addition to the expression of NK-activating ligands.

mDC TICAM-1 pathway efficiently links CTL/NK activation by mDCs. Missing the cell surface-specific TLR, TLR22, and conserving ER-resident TLR, TLR3, in mDCs may cause the functional specialization of the TICAM-1 pathway on evoking cellular immunity in mammals. Although the signaling pathway by which type I IFN is induced has been elucidated in each cell type, the exact pathway that drives NK activation or CTL induction by mDCs has not been identified.

Effector induction in transgenic mice with TLR22 for surface dsRNA recognition

Upon transfection of fgTLR22 or fgTLR3 into human or mouse cells, fgTLR22 functions as an RNA sensor for IFN induction in these mammalian cells, suggesting that mice and human TICAM-1 are compatible with fish TLR22 and TLR3 (37). With this finding in mind, we have generated TLR22 transgenic (Tg) mice to test fish TLR22 antiviral function and NK activation in mouse. TLR22 is ubiquitously expressed in all the organs tested in the Tg mice (A. Matsuo, H. Oshiumi, T. Seya, unpublished data). Its expression profile is similar to that in fish, in which endogenous fish TICAM-1 is ubiquitously expressed. PolyI:C or poliovirus were used as type I IFN inducers for *in vitro* mouse embryonic fibroblasts (MEF) stimulation studies. TLR22-expressing MEFs produce high levels of type I IFN within 6 h, a time period during which control MEFs still do not produce type I IFN. Rapid induction and three- to fivefold higher levels of IFN-β in the supernatant are characteristic features of TLR22-expressing MEFs. Similar results were obtained with BMDCs.

The levels of NK activation induced by BMDCs do not differ significantly between TLR22-expressing BMDCs and control BMDCs. We believe that TLR22 differs from TLR3 in its ability to activate cellular immune responses. However, further investigation is necessary to establish the final conclusion.

Virus infection studies were performed on Tg mice using influenza virus and poliovirus in an *in vivo* mouse model (A. Matsuo, H. Oshiumi, T. Seya, unpublished data). Both Tg and control mice died of influenza infection within 7 days. It appeared that TLR22 did not protect mice from influenza. By contrast, Tg mice expressing the poliovirus receptor (PVR) and TLR22 were relatively resistant to poliovirus infection compared with TLR22-negative control PVR-Tg mice. Wildtype mice died within 5 days, but Tg mice survived for a significant longer period. Hence, TLR22 harbors antiviral activity against acute infection of dsRNA or positive-stranded RNA viruses. This TLR22 function is conserved in TLR22-positive cells of Tg mice. We support the interpretation that TLR22 is lost in mammals so that the TLR22 supplement recovers resistance to dsRNA-generating viruses. The summary of this issue on TLR22-Tg mice is illustrated in Fig. 6.

Although cell surface activation of TLR3 or TLR22 may not be associated with induction of cellular immunity, these molecules efficiently suppress acute viral infection by generating type I IFN. Development of the endosomal RNA recognition system in mDCs would be essential in mammals for enhancing the induction of cell-mediated and long-lasting immunity in viral infection. Although to what extent TLR22 participates in the induction of cellular immunity by virus infection remains largely unsettled, fish unequivocally develop the endosomal RNA recognition system involving TLR3. Cell surface RNA recognition by TLR3 exerts some toxic features (7, 53), which may facilitate limited usage of TLR3 on membrane surface. Part of the linking between TLRs and cellular immune responses should have been established before human and fish ancestors diverged.

Prototype of the vertebrate TLR system

The phylogenetic tree of vertebrate TLR family members strongly supports the notion that non-mammalian vertebrate TLRs emerged during the Cambrian period together with other mammalian TLRs (13, 14, 36, 49); thus, the human ancestor probably possessed both contemporary TLR subsets and those of non-mammalian vertebrates. Based on our knowledge of the functional coverage of vertebrate TLR family members, the expected TLR subsets that the vertebrate

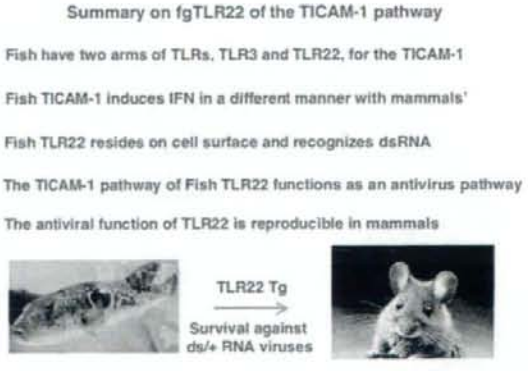

Fig. 6. Summary on fgTLR22 of the TICAM-1 pathway. (i) Fish have two arms of TLRs, TLR3, and TLR22, for the TICAM-1. (ii) Fish TICAM-1 induces IFN in a different manner with mammals. (iii) Fish TLR22 resides on cell surface and recognizes dsRNA. (iv) The TICAM-1 pathway of fish TLR22 functions as an antivirus pathway. (v) The antiviral function of TLR22 is reproducible in mammals.

common ancestor would have possessed would include at least the following 10 TLR members: TLR2, TLR3, TLR4, TLR5, TLR7, TLR8, TLR9, TLR21, TLR21, and TLR22 (13) (*Table* 1). Prior to the evolution of mammals, gene duplications would have occurred, especially in TLR2 subfamily members. Furthermore, some TLR genes were lost in some lineages, although the reason remains unknown. For example, TLR21 was diminished in the mammalian lineage, and TLR22 was lost when the mammalian ancestor began to live on land (36). Why did our human ancestor lose TLR21 and TLR22 during evolution? There are two possible explanations. First, mammals need to recognize patterns in the endosome to link the acquired responses so that non-mammalian TLRs present on the cell surface would become dispensable in the innate system. This scenario is conceivable, because the acquired system in mammals is far more sophisticated than that of teleosts. Second, the mammalian lineage happened to lose the non-mammalian TLRs. This observation is not surprising because loss of genes, which are useful for the descendant, has occurred occasionally during vertebrate evolution. For example, the vertebrate ancestor probably possessed broader spectral opsin genes for light sensing, keener auditory sensors for sound hearing, and more olfactory genes for smell sensing than humans, but the mammalian ancestor lost these outstanding genes since their divergence from reptiles (54); thus, many mammalian species are less sensitive to distal light wavelength of light, high frequency of sound, and faint smell than other non-mammalian vertebrates. If mammals had successfully reproduced TLR22 in their genomes, innate immunity in humans would have been stronger. Optional environmental pressure by pathogens may have led to the divergence of the immune system, resulting in variations. In any case, TLRs linked cellular immunity a long time ago: a common ancestor of fish and human already had a prototype. Based on this view, it appears that our immune system is not ideal but is just an example of how infections with certain pathogens have been prevented over a long time period.

References

1. Medzhitov R, Janeway CA Jr. Innate immunity: the virtues of a nonclonal system of recognition. Cell 1997;**91**:295–298.
2. Medzhitov R, Preston-Hurlburt P, Janeway CA Jr. A human homologue of the *Drosophila* Toll protein signals activation of adaptive immunity. Nature 1997;**388**:394–397.
3. Akira S, Uematsu S, Takeuchi O. Pathogen recognition and innate immunity. Cell 2006;**124**:783–801.
4. Yoneyama M, Fujita T. Function of RIG-I-like receptors in antiviral innate immunity. J Biol Chem 2007;**282**:15315–15318.
5. Matsumoto M, Seya T. TLR3: interferon induction by double-stranded RNA including poly(I:C). Adv Drug Deliv Rev 2008;**60**: 805–812.
6. Carter WA, Pitha PM, Marshall LW, Tazawa I, Tazawa S, Ts'o PO. Structural requirements of the rI n–rC n complex for induction of human interferon. J Mol Biol 1972;**70**:567–587.
7. Absher M, Stinebring WR. Toxic properties of a synthetic double-stranded RNA. Endotoxin-like properties of poly I:poly C, an interferon stimulator. Nature 1969; **223**:715–717.
8. Sasai M, Shingai M, Funami K, Yoneyama M, Fujita T, Matsumoto M, Seya T. NAK-associated protein 1 participates in both the TLR3 and the cytoplasmic pathways in type I IFN induction. J Immunol 2006;**177**: 8676–8683.
9. Honda K, Taniguchi T. IRFs: master regulators of signalling by Toll-like receptors and cytosolic pattern-recognition receptors. Nat Rev Immunol 2006;**6**:644–658.
10. Hoshino K, Kaisho T. Nucleic acid sensing Toll-like receptors in dendritic cells. Curr Opin Immunol 2008;**20**:408–413.
11. Iwasaki A, Medzhitov R. Toll-like receptor control of the adaptive immune responses. Nat Immunol 2004;**5**:987–995.
12. Reis e Sousa C. Dendritic cells in a mature age. Nat Rev Immunol 2006;**6**: 476–483.
13. Oshiumi H, Tsujita T, Shida K, Matsumoto M, Ikeo K, Seya T. Prediction of the prototype of the human Toll-like receptor gene family from the pufferfish, *Fugu rubripes*, genome. Immunogenetics 2003;**54**: 791–800.
14. Roach JC, et al. The evolution of vertebrate Toll-like receptors. Proc Natl Acad Sci USA 2005;**102**:9577–9582.
15. Baoprasertkul P, Peatman E, Somridhivej B, Liu Z. Toll-like receptor 3 and TICAM genes in catfish: species-specific expression profiles following infection with *Edwardsiella ictaluri*. Immunogenetics 2006;**58**:817–830.
16. Sullivan C, Postlethwait JH, Lage CR, Millard PJ, Kim CH. Evidence for evolving Toll-IL-1 receptor-containing adaptor molecule function in vertebrates. J Immunol 2007; **178**:4517–4527.
17. Yoneyama M, Onomoto K, Fujita T. Cytoplasmic recognition of RNA. Adv Drug Deliv Rev 2008;**60**:841–846.
18. Matsumoto M, et al. Subcellular localization of Toll-like receptor 3 in human dendritic cells. J Immunol 2003;**171**:3154–3162.
19. Ebihara T, Shingai M, Matsumoto M, Wakita T, Seya T. Hepatitis C virus-infected hepatocytes extrinsically modulate dendritic cell maturation to activate T cells and natural killer cells. Hepatology 2008;**48**: 48–58.
20. Fan S, et al. Zebrafish TRIF, a Golgi-localized protein, participates in IFN induction and NF-kappaB activation. J Immunol 2008;**180**:5373–5383.
21. Matsumoto M, Kikkawa S, Kohase M, Miyake K, Seya T. Establishment of a monoclonal antibody against human Toll-like receptor 3 that blocks double-stranded RNA-mediated signaling. Biochem Biophys Res Commun 2002;**293**:1364–1369.
22. Funami K, Matsumoto M, Oshiumi H, Akazawa T, Yamamoto A, Seya T. The cytoplasmic 'linker region' in Toll-like receptor 3 controls receptor localization and signaling. Int Immunol 2004;**16**:1143–1154.
23. de Bouteiller O, et al. Recognition of double-stranded RNA by human toll-like receptor 3 and downstream receptor signaling requires multimerization and an acidic pH. J Biol Chem 2005;**280**:38133–38145.
24. Oshiumi H, Matsumoto M, Funami K, Akazawa T, Seya T. TICAM-1, an adaptor molecule that participates in Toll-like receptor 3-mediated interferon-beta induction. Nat Immunol 2003;**4**:161–167.

25. Yamamoto M, et al. Role of adaptor TRIF in the MyD88-independent toll-like receptor signaling pathway. Science 2003;**301**: 640–643.
26. Häcker H, et al. Specificity in Toll-like receptor signalling through distinct effector functions of TRAF3 and TRAF6. Nature 2006;**439**:204–207.
27. Oganesyan G, et al. Critical role of TRAF3 in the Toll-like receptor-dependent and -independent antiviral response. Nature 2006;**439**:208–211.
28. Sharma S, tenOever BR, Grandvaux N, Zhou GP, Lin R, Hiscott J. Triggering the interferon antiviral response through an IKK-related pathway. Science 2003;**300**: 1148–1151.
29. Fitzgerald KA, et al. IKKepsilon and TBK1 are essential components of the IRF3 signaling pathway. Nat Immunol 2003;**4**:491–496.
30. Akazawa T, et al. Antitumor NK activation induced by the Toll-like receptor 3-TICAM-1 (TRIF) pathway in myeloid dendritic cells. Proc Natl Acad Sci USA 2007;**104**:252–257.
31. Schulz O, et al. Toll-like receptor 3 promotes cross-priming to virus-infected cells. Nature 2005;**433**:887–892.
32. Meylan E, Burns K, Hofmann K, Blancheteau V, Martinon F, Kelliher M, Tschopp J. RIP1 is an essential mediator of Toll-like receptor 3-induced NF-kappa B activation. Nat Immunol 2004;**5**:503–507.
33. Salem ML, Kadima AN, Cole DJ, Gillanders WE. Defining the antigen-specific T-cell response to vaccination and poly(I:C)/TLR3 signaling: evidence of enhanced primary and memory CD8 T-cell responses and antitumor immunity. J Immunother 2005;**28**: 220–228.
34. Sivori S, et al. CpG and double-stranded RNA trigger human NK cells by Toll-like receptors: induction of cytokine release and cytotoxicity against tumors and dendritic cells. Proc Natl Acad Sci USA 2004;**101**: 10116–10121.
35. Salaun B, Coste I, Rissoan MC, Lebecque SJ, Renno T. TLR3 can directly trigger apoptosis in human cancer cells. J Immunol 2006;**176**:4894–4901.
36. Oshiumi H, Matsuo A, Matsumoto M, Seya T. Pan-vertebrate Toll-like receptors during evolution. Curr Genomics 2008;**9**:488–493.
37. Matsuo A, et al. Teleost TLR22 recognizes RNA duplex to induce IFN and protect cells from birnaviruses. J Immunol 2008;**181**:3474–3485.
38. Funami K, Sasai M, Ohba Y, Oshiumi H, Seya T, Matsumoto M. Spatiotemporal mobilization of TICAM-1 in response to dsRNA. J Immunol 2007;**179**: 6827–6830.
39. Funami K, Sasai M, Oshiumi H, Seya T, Matsumoto M. Homo-oligomerization is essential for Toll/IL-1 receptor domain containing adaptor molecule-1 signaling. J Biol Chem 2008;**283**:18283–18291.
40. Bergan V, Steinsvik S, Xu H, Kileng Ø, Robertsen B. Promoters of type I interferon genes from Atlantic salmon contain two main regulatory regions. FEBS J 2006; **273**:3893–3906.
41. Rudd BD, et al. Deletion of TLR3 alters the pulmonary immune environment and mucus production during respiratory syncytial virus infection. J Immunol 2006; **176**:1937–1942.
42. Harada K, et al. Innate immune response to double-stranded RNA in biliary epithelial cells is associated with the pathogenesis of biliary atresia. Hepatology 2007;**46**: 1146–1154.
43. Cario E, Podolsky DK. Differential alteration in intestinal epithelial cell expression of toll-like receptor 3 (TLR3) and TLR4 in inflammatory bowel disease. Infect Immun 2000;**68**:7010–7017.
44. Nakamura MK, et al. Increased expression of TLR3 in human intrahepatic biliary epithelial cells at the site of ductular reaction in primary billiary cirrhosis. Hepatol Intern 2008;**2**:222–230.
45. Phelan PE, Pressley ME, Witten PE, Mellon MT, Blake S, Kim CH. Characterization of snakehead rhabdovirus infection in zebrafish (*Danio rerio*). J Virol 2005;**79**:1842–1852.
46. Nishizawa T, Kinoshita S, Yoshimizu M. An approach for genogrouping of Japanese isolates of aquabirnaviruses in a new genogroup, VII, based on the VP2/NS junction region. J Gen Virol 2005;**86**:1973–1978.
47. Ando T, Suzuki H, Nishimura S, Tanaka T, Hiraishi A, Kikuchi K. Characterization of extracellular RNAs produced by the marine photosynthetic bacterium *Rhodovulum sulfidophilum*. J Biochem 2006;**139**:805–811.
48. Coulibaly F, et al. The birnavirus crystal structure reveals structural relationships among icosahedral viruses. Cell 2005;**120**:761–772.
49. Ishii A, Kawasaki M, Matsumoto M, Tochinai S, Seya T. Phylogenetic and expression analysis of amphibian *Xenopus* Toll-like receptors. Immunogenetics 2007;**59**:281–293.
50. Akazawa T, et al. Tumor immunotherapy using bone marrow-derived dendritic cells overexpressing Toll-like receptor adaptors. FEBS Lett 2007;**581**:3334–3340.
51. Akazawa T, et al. Adjuvant-mediated tumor regression and tumor-specific cytotoxic response are impaired in MyD88-deficient mice. Cancer Res 2004;**64**:757–764.
52. Seya T, Akazawa T, Uehori J, Matsumoto M, Azuma I, Toyoshima K. Role of toll-like receptors and their adaptors in adjuvant immunotherapy for cancer. Anticancer Res 2003;**23**:4369–4376.
53. Zhou R, Wei H, Sun R, Tian Z. Recognition of double-stranded RNA by TLR3 induces severe small intestinal injury in mice. J Immunol 2007;**178**:4548–4556.
54. International Human Genome Sequencing Consortium. Finishing the euchromatic sequence of the human genome. Nature 2004;**431**:931–945.

THE JOURNAL OF BIOLOGICAL CHEMISTRY VOL. 284, NO. 2, pp. 807–817, January 9, 2009

Riplet/RNF135, a RING Finger Protein, Ubiquitinates RIG-I to Promote Interferon-β Induction during the Early Phase of Viral Infection*[S]

Received for publication, June 3, 2008, and in revised form, November 10, 2008 Published, JBC Papers in Press, November 18, 2008, DOI 10.1074/jbc.M804259200

Hiroyuki Oshiumi[‡], Misako Matsumoto[‡], Shigetsugu Hatakeyama[§], and Tsukasa Seya[‡1]

From the [‡]Department of Microbiology and Immunology and the [§]Department of Biochemistry, Hokkaido University Graduate School of Medicine, Kita-15, Nishi-7, Kita-ku Sapporo 060-8638, Japan

RIG-I (retinoic acid-inducible gene-I), a cytoplasmic RNA helicase, interacts with IPS-1/MAVS/Cardif/VISA, a protein on the outer membrane of mitochondria, to signal the presence of virus-derived RNA and induce type I interferon production. Activation of RIG-I requires the ubiquitin ligase, TRIM25, which mediates lysine 63-linked polyubiquitination of the RIG-I N-terminal CARD-like region. However, how this modification proceeds for activation of IPS-1 by RIG-I remains unclear. Here we identify an alternative factor, Riplet/RNF135, that promotes RIG-I activation independent of TRIM25. The Riplet/RNF135 protein consists of an N-terminal RING finger domain, C-terminal SPRY and PRY motifs, and shows sequence similarity to TRIM25. Immunoprecipitation analyses demonstrated that the C-terminal helicase and repressor domains of RIG-I interact with the Riplet/RNF135 C-terminal region, whereas the CARD-like region of RIG-I is dispensable for this interaction. Riplet/RNF135 promotes lysine 63-linked polyubiquitination of the C-terminal region of RIG-I, modification of which differs from the N-terminal ubiquitination by TRIM25. Overexpression and knockdown analyses revealed that Riplet/RNF135 promotes RIG-I-mediated interferon-β promoter activation and inhibits propagation of the negative-strand RNA virus, vesicular stomatitis virus. Our data suggest that Riplet/RNF135 is a novel factor of the RIG-I pathway that is involved in the evoking of human innate immunity against RNA virus infection, and activates RIG-I through ubiquitination of its C-terminal region. We infer that a variety of RIG-I-ubiquitinating molecular complexes sustain RIG-I activation to modulate RNA virus replication in the cytoplasm.

Cytoplasmic viral RNA sensors induce production of type I interferon (IFN)[2] (1, 2). Representative cytoplasmic sensors, RIG-I-like receptors (RLRs) of RIG-I, MDA5, and LGP2, belong to the DEA(D/H) box RNA helicase family (3–6). RIG-I recognizes the 5′ end triphosphate of the virus RNA genome or double-stranded RNA (6–8) to sense infection by various RNA viruses (3, 5). The RIG-I protein consists of two N-terminal CARD-like domains, an RNA helicase region and a repressor domain (RD) (9). After recognition of positive or negative single-stranded viral RNA, RIG-I interacts with its adaptor molecule IPS-1/MAVS/Cardif/VISA leading to type I IFN production, thereby protecting host cells from amplified viral replication (10–13). However, only a few copies of viral RNAs usually penetrate the cell membrane to enter the cell at an early infection, and these RLRs are barely present in intact as well as early virus-infected cells (6). The early viral RNA recognition facility should be different from that of the late phase when RIG-I protein is abundant in the cytoplasm and easily re-organizes the virus RNAs. What molecular mechanism is responsible for initial sensing of viral RNA thus remains unknown.

Other RLRs, MDA5 and LGP2, are structurally similar to RIG-I in their having the helicase domain (5, 14). However, MDA5 lacks the RD domain although it possesses CARD-like region at the N terminus like RIG-I. LGP2 does not have a CARD-like region but possesses RD at its C terminus (9). RIG-I and MDA5 recognize different kinds of RNA viruses and in some cases play a redundant role in sensing virus infection, such as influenza B (15). In contrast, LGP2 rather negatively regulates virus replication. LGP2 expression suppressed RIG-I or MDA5 signaling (14, 16), and *lgp2* gene disruption conferred high susceptibility to virus infection on mice (4).

Recently, the majority of proteins involved in the type I IFN-inducing system were found ubiquitinated. For example, the tumor necrosis factor receptor-associated family members, TRAF3 and TRAF6, are ubiquitin ligases to induce ubiquitination of proteins and implicated in activation of IFN regulatory factor (IRF) 3 or nuclear factor (NF) κB (13, 17–19). In contrast, a deubiquitinating enzyme, DUBA or A20, suppresses these signals (19, 20). In addition to ubiquitin, ubiquitin-like protein, ISG15, is also conjugated to proteins involved in the IFN-inducing pathway (21, 22). Recent studies have revealed that viral RNA sensors are also ubiquitinated. TRIM25 (ZNF147 or EFP), a member of the ubiquitin-protein isopeptide ligase family, which possesses a RING finger domain, ubiquitinates the

* This work was supported in part by grants-in-aid from the Ministry of Education, Science and Culture of Japan, Ministry of Health, Labour, and Welfare, The Mitsubishi Foundation, and The Mochida Memorial Foundation. The costs of publication of this article were defrayed in part by the payment of page charges. This article must therefore be hereby marked "*advertisement*" in accordance with 18 U.S.C. Section 1734 solely to indicate this fact.

[S] The on-line version of this article (available at http://www.jbc.org) contains supplemental Figs. S1–S6.

The nucleotide sequence(s) reported in this paper has been submitted to the GenBank™/EBI Data Bank with accession number(s) AB470605.

[1] To whom correspondence should be addressed: Dept. of Microbiology and Immunology, Graduate School of Medicine, Hokkaido University, Kita-ku, Sapporo 060-8638, Japan. Tel.: 81-11-706-5073; Fax: 81-11-706-7866; E-mail: seya-tu@pop.med.hokudai.ac.jp.

[2] The abbreviations used are: IFN, interferon; RT, reverse transcription; RLR, RIG-I-like receptor; HA, hemagglutinin; siRNA, small interference; m.o.i., multiplicity of infection; VSV, vesicular stomatitis virus; IRF, IFN regulatory factor; Ub, ubiquitin; ORF, open reading frame; RD, repressor domain.

CARD-like domains of RIG-I thereby facilitating the RIG-I-mediated activation of type I IFN signaling (23, 24), although Shimotohno and co-workers (25) previously reported that TRIM25 (EFP) does not polyubiquitinate the RIG-I CARD-like region as far under their conditions. Expression of TRIM25 increases RIG-I CARD-like region-mediated signaling; however, it remains to be determined whether the activation of full-length RIG-I requires other ubiquitin ligase (23). Another ubiquitin ligase RNF125 mediates lysine 48-linked polyubiquitination of RIG-I, which leads to degradation of RIG-I through the proteasome (25).

Here we examined what molecular complex participates in an early RIG-I-mediated RNA recognition and IFN signaling by yeast two-hybrid screening. Here we detected two novel RING finger proteins that bound to RIG-I, and we found that one, RNF135, facilitated RIG-I-mediated type I IFN induction via ubiquitinating RIG-I. RNF135 plays a crucial role in the RIG-I response to minimal copies of viral RNA, and by binding to the C-terminal helicase and RD regions of RIG-I, RNF135 facilitates RIG-I C-terminal ubiquitination to up-regulate RIG-I-mediated IFN signaling and suppress viral replication. Hence, we renamed it as RNF135 Riplet (RING finger protein leading to RIG-I activation). To our knowledge, this is the first study demonstrating that C-terminal ubiquitination of RIG-I is important for full IFN induction by RIG-I.

EXPERIMENTAL PROCEDURES

Cell Cultures—HEK293 and Vero cells were cultured in Dulbecco's modified Eagle's medium with 10% fetal calf serum (Invitrogen), and HeLa cells were in minimum Eagle's medium with 2 mM L-glutamine and 10% fetal calf serum (JRH Biosciences). HEK293FT cells were maintained in Dulbecco's modified Eagle's high glucose medium containing 10% heat-inactivated fetal calf serum (Invitrogen).

Plasmids—cDNA fragment encoding a C-terminal region of Riplet was isolated by yeast two-hybrid screening using human lung cDNA library. The 5′ region encoding the remaining N-terminal region was amplified by PCR using primers Riplet-F1 and Riplet-R1, and human lung cDNA library was used for its template. Two cDNA fragments, which cover the entire ORF of Riplet, were joined by PCR using primers Riplet-F1, R1, F2, and R2 and then inserted into pCR-blunt vector (Invitrogen). The primers sequences are as follows: F1, GCCTCGAGGCCACCATGGCGGGCCTGGGCCTGGG; R1, CGGCCAGGTCCTGCAGTAGC; F2, GCACCTGCGGAAGAACACGC; and R2, GGGGATCCCACCTTTACTTGCTTTATTATCAGG. The obtained cDNA was cloned into XhoI-NotI restriction sites of pEF-BOS expression vector, and the HA tag was fused at the C-terminal end of Riplet. Riplet-DN (dominant negative) expression vector was constructed by amplifying the relevant Riplet cDNA fragment using the primers Riplet-X-F-C and Riplet-R2 and subcloned into pEF-BOS. The primer sequence of Riplet-X-F-C was as follows: GCTCGAGGCCACCATGCCGCACCTGCGGAAGAACACGC. Riplet-L248fs expression vector was made by deleting 1 base at position 742 by standard PCR-mediated site-directed mutagenesis methods with primers Riplet-L248fs-F and Riplet-L248fs-R as follows: Riplet-L248fs-F, CCAGAGCCACCCTGCATCAGGAGAGCTTCTCGG, and Riplet-L248fs-R, CCGAGAAGCTCTCCTGATGCAGGGTGGCTCTGG. All cloned *RIPLET* cDNA fragments were sequenced, and it was confirmed that there were no mutations. Full-length RIG-I expressing vector, Gal4-IRF-3, Gal4-DBD, and p55 UASG-Luc reporter plasmids were gifts from Dr. T. Fujita (Kyoto University, Kyoto, Japan). p125 luc reporter plasmid was a gift from Dr. T. Taniguchi (University of Tokyo, Tokyo, Japan). RIG-I RD expressing vector was made with primers RIG-I RD-F and RIG-I RD-R; the RIG-I dRD cDNA fragment, which encodes ORF of RIG-I from the 1- to 754-amino acid region, was made by using primers RIG-I-(1–754)F and RIG-I-(1–754)R. The obtained cDNA fragments were sequenced, and it was confirmed that there were no mutations caused by PCR. The primers sequences are as follows: RIG-I RD-F, GAT GAT AAA GGT ACC ACC GGT AGC AAG TGC TTC CTT CTG; RIG-I RD-R, AAG GAA GCA CTT GCT ACC GGT GGT ACC TTT ATC ATC ATC ATC; RIG-I-(1–754)F, GC AGA GGA AGA GCA AGA TGA TAT CAG GTC CTC AAT CTT C; and RIG-I-(1–754)R, ATT GAG GAC CTG ATA TCA TCT TGC TCT TCC TCT GCC TC.

Northern Blotting—Human *RIPLET* 1092-bp cDNA fragment (208–1299) was used for the probe for Northern blotting. The Northern blot membranes, human 12-lane MTN blot and MTN blot III, were purchased from Clontech. The homology of human *RIPLET* and *TRIM25* in the probe region was 46%. We used a stringent condition for Northern blotting to exclude the cross-hybridization between the *RIPLET* and *TRIM25* genes. Briefly, the probe was labeled with [α-^{32}P]dCTP using Rediprime II Random Prime labeling system (GE Healthcare). The labeled probe was hybridized to the membrane with ExpressHyb hybridization solution (Clontech) at 68 °C for 1 h. The membrane was washed with washing solution I (2× SSC, 0.05% SDS) for 40 min, and then washed with washing solution II (0.1× SSC, 0.1% SDS) for 40 min. Riplet mRNA bands were detected with x-ray film.

Reporter Gene Analysis—HEK293 cells were transiently transfected in 24-well plates using FuGENE HD (Roche Applied Science) with expression vectors, reporter plasmids, and internal control plasmid coding *Renilla* luciferase. The total amounts of plasmids were normalized with empty vector. For poly(I-C) stimulation, 24 h after transfection, cells were stimulated with medium containing poly(I-C) (50 μg/ml) and DEAE-dextran (0.5 mg/ml) for 1 h, and then the medium was exchanged with normal medium and incubated for an additional 3 h. Cells were lysed with lysis buffer (Promega) and luciferase, and *Renilla* luciferase activities were measured by the dual luciferase assay kit (Promega). Relative luciferase activities were calculated by normalizing luciferase activity by *Renilla* luciferase activity, and dividing the normalized value by control in which only empty vector, reporter, and internal control plasmid were transfected. Values are expressed as mean relative stimulations ± S.D. for a representative experiment, and each was performed three times in duplicate (unless otherwise indicated in the legends).

RNA Interference—Reporter and siRNA (20 nM final concentration) for Riplet or control were transfected into HEK293 cells with Lipofectamine 2000 (Invitrogen) by the standard method described in the manufacturer's protocol. Empty vec-

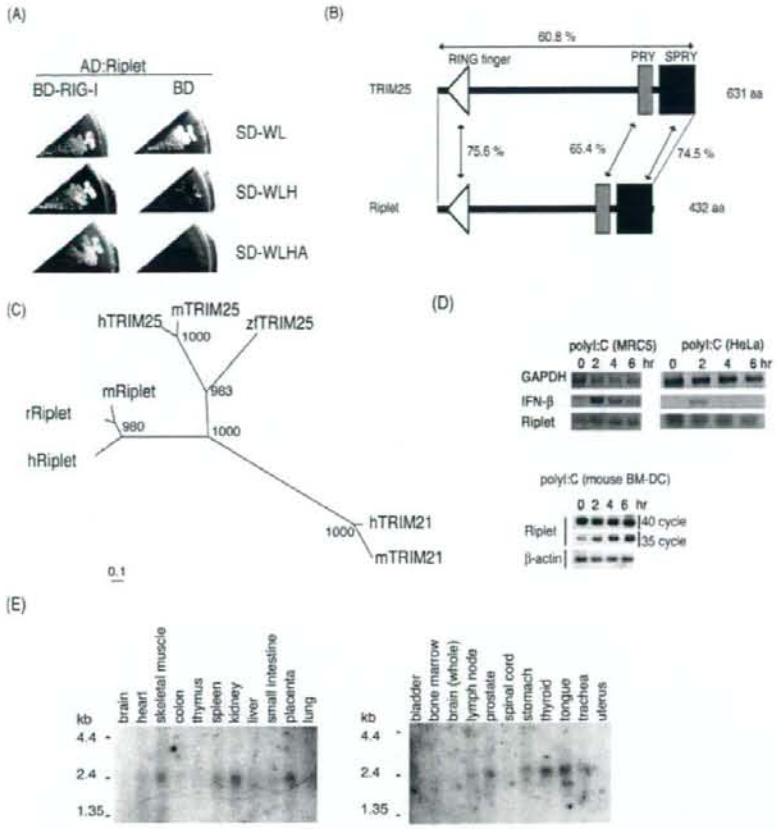

FIGURE 1. **Isolation of Riplet by yeast two-hybrid screening.** *A*, yeast cells carrying both RIG-I and Riplet can grow in selective media (SD-WLH, SD-WLHA), whereas yeast cells carrying RIG-I alone only grow in nonselective media (SD-WL), indicating the physical interaction of RIG-I with Riplet. *B*, human Riplet protein sequence is 60.8% identical to human TRIM25. The RING finger domains and SPRY motifs show higher sequence similarities between the two proteins. *aa*, amino acids. *C*, phylogenetic tree constructed by the Neighbor-Joining method shows that Riplet is similar to TRIM25. *h*, *m*, *r*, or *zf* represent human, mouse, rat, or zebrafish, respectively. The *numbers* on the node are bootstrap probabilities (n = 1000). *D*, HeLa cell, human primary-cultured fibroblast cell, MRC5, or bone marrow-derived mouse dendritic cell (*BM-DC*) were stimulated with poly(I-C) (50 μg/ml) for indicated hours. Total RNA was extracted with TRIzol reagent, and then RT-PCR was carried out using primers shown under "Experimental Procedures." *GAPDH*, glyceraldehyde-3-phosphate dehydrogenase. *E*, Northern blot membranes containing 1 μg of poly(A)$^+$ RNA per lane from human tissues were blotted with human Riplet probe.

tor was added to normalize the final plasmid amount. 48 h after transfection, cells were stimulated with poly(I-C) for 4 h. For VSV infection, 24 h after transfection, cells were infected with VSV at m.o.i. = 1, and cell lysate was prepared after 12 h for reporter gene assays. The degree of gene silencing was confirmed by RT-PCR using RNA extracted from cells 24 h after transfection. PCR primers used for the RT-PCR were Riplet-F3 (ACTGGGAAGTGGACACTAGG) and Riplet-R3 (ACTCATACAGAAGCTTCTCC). siRNAs were purchased from Funakoshi Co., Ltd. (Tokyo Japan), and the siRNA sequences of Riplet siRNA were GACUAUGGACUCUUGUUGUGU (sense) and ACAACAAGAGUCCAUAGUCCU (antisense). Control siRNA sequences were CUGUUGGUUUAGUAAGCCUGU (sense) and AGGCUUACUAAACCAACAGUC (antisense). Another siRNA, Riplet si-1, and control negative siRNA (silencer negative control 1 siRNA, AM4611) were purchased from Applied Biosystems. siRNA sequences were Riplet si-1 GGGAAAGCUUGCCUUCUAUdTdT (sense) and AUAGAAGGCAAGCUUUCCCdTdC (antisense).

Virus Preparation and Infection—VSV Indiana strain and poliovirus were amplified using Vero cells. HEK293 cells were transfected in 24-well plates with plasmid encoding *RIG-I*, Riplet, or no insert. 24 h after transfection, cells were infected with viruses for 24 h, and the titers of virus in culture supernatant were measured by plaque assay using Vero cells. For RNA interference assay, cells were transfected with siRNA with Lipofectamine 2000. 24 h after transfection, cells were infected with viruses at m.o.i. = 0.001 for 18 h, and the titer in culture supernatant were determined by plaque assay.

Immunoprecipitation—HEK293FT cells were transfected in 6-well plates with plasmids encoding FLAG-tagged RIG-I and/or HA-tagged Riplet. The plasmid amounts were normalized by the addition of empty plasmid. 24 h after transfection, cells were lysed with lysis buffer (20 mM Tris-HCl (pH 7.5), 125 mM NaCl, 1 mM EDTA, 10% glycerol, 1% Nonidet P-40, 30 mM NaF, 5 mM Na_3VO_4, 20 mM iodoacetamide, and 2 mM phenylmethylsulfonyl fluoride), and then proteins were immunoprecipitated with rabbit anti-HA polyclonal (Sigma) or anti-FLAG M2 monoclonal antibody (Sigma). The precipitated samples were analyzed by SDS-PAGE and stained with anti-HA (HA1.1) (Covance) or anti-FLAG M2 monoclonal antibody. For ubiquitination assay of RIG-I, the plasmid encoding two multiple HA-tagged ubiquitins was used. HEK293FT cells were transfected with plasmids encoding FLAG-tagged RIG-I, Riplet, or 2× HA-tagged ubiquitin. 24 h after transfection, cells were lysed, and then RIG-I was immunoprecipitated as described above. The samples were analyzed by SDS-PAGE and stained with anti-HA polyclonal antibody (for detection of ubiquitination) or anti-FLAG monoclonal antibody (for detection of RIG-I). Reproducibility was confirmed with additional experiments (see supplemental figures).

Construction of RIG-I 3KA and 5KA Mutant Genes—The C-terminal three or five lysine residues were mutated into alanines (designated as 3KA and 5KA). RIG-I 3KA has K888A, K907A, and K909A, whereas RIG-I 5KA has K849A, K851A,

K888A, K907A, and K909A. The mutant *rig-I* genes were made by PCR-mediated site-directed mutagenesis. The primers used for the PCR were as follows: K907–909A-forward, GTT CAG ACA CTG TAC TCG GCG TGG GCG GAC TTT CAT TTT GAG AAG, and K907–909A-reverse, CTT CTC AAA ATG AAA GTC CGC CCA CGC CGA GTA CAG TGT CTG AAC; K888A-forward, GAC ATT TGA GAT TCC AGT TAT AGC AAT TGA AAG TTT TGT GGT GGA GG, and K888A-reverse, CCT CCA CCA CAA AAC TTT CAA TTG CTA TAA CTG GAA TCT CAA ATG TC; K849–851A-forward, GAG TAG ACC ACA TCC CGC CCA GCG CAG TTT TCA AGT TTT G, and K849–851A-reverse, CAA AAC TTG AAA ACT GCG CTG GCG CGG GAT GTG GTC TAC TC. PCR was carried with Pyrobest *Taq* polymerase, and the obtained clones were sequenced to exclude the clones harboring PCR error. To construct the plasmid-expressing mutant RIG-I protein, the wild-type *RIG-I* gene on pEF-BOS vector was replaced with the mutant *rig-I* gene.

Real Time PCR—Quantitative PCR analyses were carried out using iCycler iQ real time detection system with Platinum SYBR Green qPCR SuperMix-UDG reagent (Invitrogen). Primer sequences for qPCR were as follows: hGAPDH-qF, GAG TCA ACG GAT TTG GTC GT, and hGAPDH-qR, TTG ATT TTG GAG GGA TCT CG; hIFN-β-qF, TGG GAG GAT TCT GCA TTA CC, and hIFN-β-qR, CAG CAT CTG CTG GTT GAA GA; hMx1-qF, ACC ACA GAG GCT CTC AGC AT, and hMx1-qR, CTC AGC TGG TCC TGG ATC TC; and hIFIT-1-qF, GCA GCC AAG TTT TAC CGA AG, and hIFIT-1-qR, CAC CTC AAA TGT GGG CTT TT. Values were expressed as mean relative stimulations, and for a representative experiment from a minimum of three separate experiments, each was performed in triplicate.

RESULTS

RIG-I-binding Proteins—To isolate the proteins that bind to RIG-I, we performed yeast two-hybrid screening using a human lung cDNA library. Using the RIG-I central region (213–601 amino acids), we isolated a clone that encoded a partial ORF of a gene expressed in a dendritic cell line, DC12, whereas the C-terminal region of RIG-I (557–925 amino acids) resulted in the isolation of two cDNA clones, which encoded partial C-terminal regions of ZNF598 and RNF135 (Fig. 1*A* and data not shown). Preliminary expression studies showed that the RNF135 segment affected the RIG-I IFN-β inducing activity, whereas the other two proteins had no effect (data not shown). We confirmed the

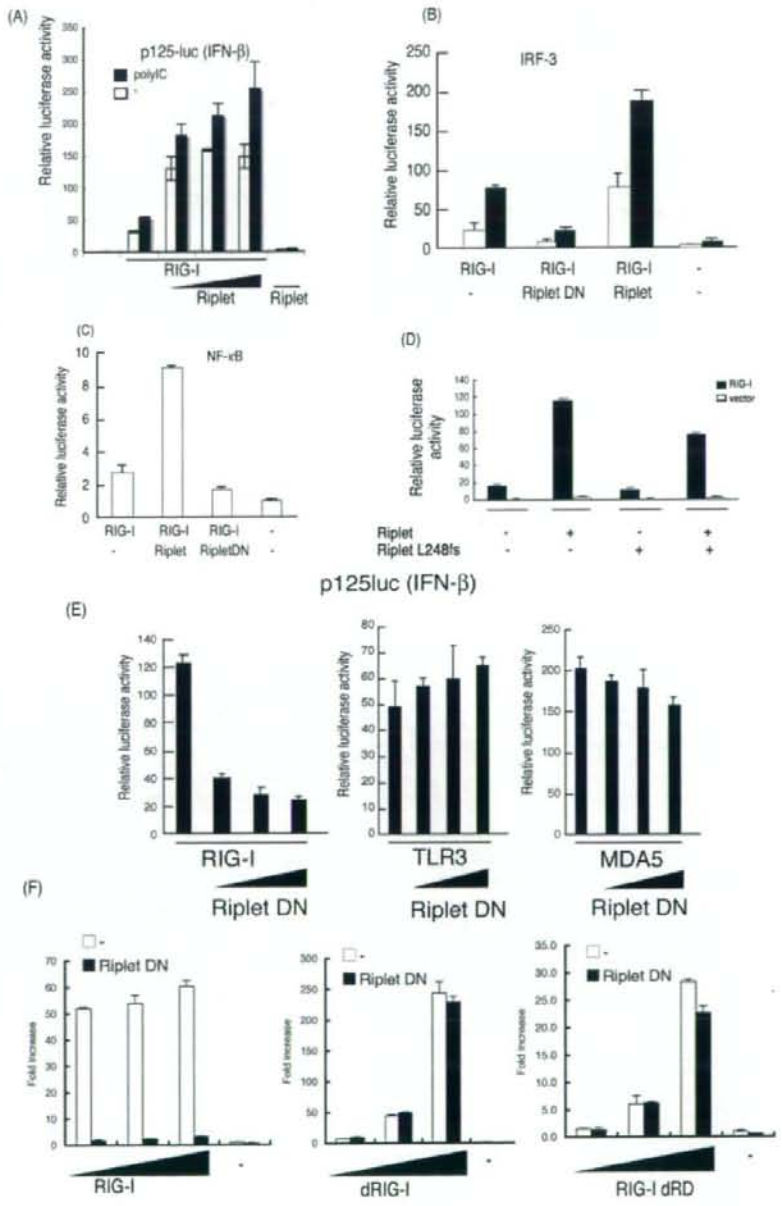

interaction of RIG-I with ZNF598 or RNF135 in HEK293FT cells by immunoprecipitation (data not shown). RNF135 was previously annotated by the genome project and was recently found to be a cause of a genetic disease, neurofibromatosis, although its protein function was unknown. We renamed the protein Riplet (RING finger protein leading to RIG-I activation) based on the following functional analyses. Riplet was most similar to TRIM25 (60.8% sequence homology), in particular between their RING finger domains PRY or SPRY (Fig. 1*B*). Phylogenetic analysis also supported the notion that Riplet was similar to TRIM25 (Fig. 1*C*). Thus, we hypothesized that, like TRIM25, Riplet is a ubiquitin ligase.

Expression of Riplet—RIG-I mRNA is induced by type I IFN or poly(I-C) stimulation in mammalian cells. Unlike RIG-I, however, Riplet mRNA was basally expressed in HeLa and primary-cultured MRC-5 cells irrespective of stimulation (Fig. 1*D* and data not shown). On the other hand, when we treated bone marrow-derived dendritic cells with poly(I-C), the basal level of Riplet mRNA was increased by the stimulation (Fig. 1*D*), suggesting that the regulatory mechanism of Riplet expression somewhat differs among cell types, and that Riplet is expressed before virus infection in some cell types. Next we performed Northern blotting of human tissue RNA. Riplet mRNA was detected as a single band of 2.4 kbp, which is slightly longer than the RNF135 cDNA sequence deposited in GenBank™ (accession number AB470605). Human *RIPLET* is expressed in human skeletal muscle, spleen, kidney, placenta, prostate, stomach, thyroid, and tongue and also weakly expressed in heart thymus, liver, and lung (Fig. 1*E*).

Riplet Enhances RIG-I-mediated IFN-β Induction—At first we characterized the role of Riplet in RIG-I-mediated IFN inducing signaling by reporter gene analyses. When RIG-I was expressed in HEK293 cells, reporter auto-activation was observed even in the absence of exogenous stimulation (Fig. 2*A*) as reported previously (25, 26). Stimulation with poly(I-C) further enhanced the promoter. Co-expression of Riplet with RIG-I potentiated activation of the IFN-β promoter, whereas expression of Riplet alone resulted in only marginal activation (Fig. 2*A*). Detection of endogenous IFN-β mRNA confirmed that Riplet enhanced RIG-I-mediated activation of IFN-β transcription (supplemental Fig. S1). The enhancing role of Riplet in IFN-β promoter activation was also supported by activation of IRF-3 and NF-κB by Riplet (Fig. 2, *B* and *C*). In contrast, expression of a Riplet partial fragment (Riplet-DN) (70–432 amino acids) that lacked the N-terminal RING finger domain reduced promoter activation (Fig. 2*E*). The Riplet-L249fs mutant protein, which was isolated from neurofibromatosis patients (27), did not increase the RIG-I-mediated promoter activation (Fig. 2*D*). These data indicate that Riplet augments RIG-I-mediated IFN-β promoter activation, and that both the RING finger domain and the C-terminal region encoding the SPRY and PRY motifs are important for its function. Riplet (residues 70–432) acted as a dominant-negative form (hereafter called Riplet-DN) (Fig. 2, *E* and *F, left panel*). This functional feature of Riplet-DN was confirmed in Fig. 2, *B* and *C*, and was later confirmed through RIG-I co-precipitation and ubiquitination analyses (see Fig. 5*C* and supplemental Fig. S4*C*). Expression of Riplet-DN did not reduce TLR3 or MDA5 signaling (Fig. 2*E*), suggesting that Riplet-DN is specific for RIG-I signaling. Interestingly, the Riplet-DN only partially suppressed the function of the C-terminal deleted RIG-I (dRD), which is a constitutively active form (Fig. 2*F, right panel*), and RIG-I CARD-like region (dRIG-I)-mediated signaling in high or low dose transfection of dRIG-I was barely inhibited by overexpression of Riplet-DN (Fig. 2*F, center panel*). These data suggest that Riplet requires the RIG-I C-terminal domain (RD) and partial helicase region to activate RIG-I signaling.

Endogenous Riplet Promotes the RIG-I Signaling—We performed Riplet knockdown by siRNA Riplet using Lipofectamine 2000 reagents, instead of FuGENE HD, to reveal the function of endogenous Riplet. Two siRNAs (Riplet siRNA and Riplet si-1) that target different sites of the Riplet mRNA and two control siRNAs were used for knockdown analyses. The two siRNA or control siRNA were co-transfected with HA-tagged Riplet expression vector into HEK293 cells, and after 48 h, cell lysate was prepared and analyzed by Western blotting with anti-HA antibody detecting Riplet. The two siRNAs targeting Riplet abolished exogenously expressed Ripelt-HA, but control siRNA did not (supplemental Fig. S3). Likewise, both Riplet siRNA and Riplet si-1 specifically down-regulate the level of endogenous Riplet mRNA (Fig. 3, *A* and *B*).

Using the siRNA, we examined whether Riplet knockdown reduces RIG-I signaling. As expected, RIG-I-mediated IFN-β promoter activation was reduced by Riplet siRNA or Riplet si-1 compared with control siRNA (Fig. 3, *A* and *B*), indicating that Riplet is required for full activation of the RIG-I signaling. Vesicular stomatitis virus (VSV) is a negative-stranded RNA virus that induces IFN-β production via RIG-I (3). Although the

FIGURE 2. **Riplet enhances IFN-β signaling mediated by RIG-I.** *A*, Riplet enhances the promoter activation by RIG-I. HEK293 cells were transfected with plasmids encoding empty vector, RIG-I (0.1 μg) and Riplet (0.025, 0.05, or 0.1 μg) together with p125-luc (IFN-β promoter) reporter plasmid in 24-well plates. 24 h after transfection, the cells were treated with mock or poly(I-C) (50 μg/ml) for 4 h as described under "Experimental Procedures," and then luciferase activities of cell lysates were measured. *Closed* or *open boxes* represent poly(I-C) or mock stimulation, respectively. *B*, to examine the activation of IRF-3, RIG-I (0.1 μg), Riplet (0.1 μg), and/or Riplet-DN (0.1 μg),expressing vectors were transfected into HEK293 cells with reporter plasmids, GAL4 fused IRF-3 (0.05 μg), and the p55 UASG-luc reporter gene (0.05 μg), in which luciferase reporter gene is fused downstream of GAL4 protein-binding site, and therefore activated IRF-3 promotes the transcription of luciferase reporter gene. The cells were stimulated with poly(I-C) as described above (34). The total amount of transfected DNA (0.5 μg/well) was kept constant by adding empty vector (pEF-BOS). *C*, HEK293 cells were transfected with RIG-I (0.1 μg), Riplet (0.1 μg), and/or Riplet-DN (0.1 μg) expressing vectors together with the NF-κB reporter plasmid (0.1 μg), and 24 h later, the luciferase activities of cell lysates were measured. *D*, Riplet-L248fs, which lacks the C-terminal region, did not enhance the activation at all. HEK293 cells were transfected with the plasmids expressing wild-type Riplet (0.1 μg) or Riplet-L248fs (0.1 μg) together with RIG-I expressing vector (0.1 μg) and p125-luc reporter (0.1 μg). 24 h after transfection, cell were stimulated with poly(I-C), and the luciferase activities of cell lysates were determined as described above. *E*, RIG-I (0.1 μg), MDA5 (0.1 μg), or TLR3 (0.1 μg) expressing vectors were transfected into HEK293 cells with the plasmid encoding the Riplet-DN fragment (0.1, 0.2, or 0.3 μg) in 24-well plates. After 24 h, the cells were stimulated with 50 μg of poly(I-C) for 4 h, and relative luciferase activities were determined. *F*, Riplet-DN (100 ng) was co-transfected with full-length RIG-I (0, 50, 100, or 200 ng), RIG-I CARD-like region (dRIG-I) (0, 50, 100, or 200 ng), or C-terminal deleted RIG-I (RIG-I dRD) (0, 50, 100, or 200 ng) into HEK293 cells in 24-well plate, and reporter gene assays were carried out.

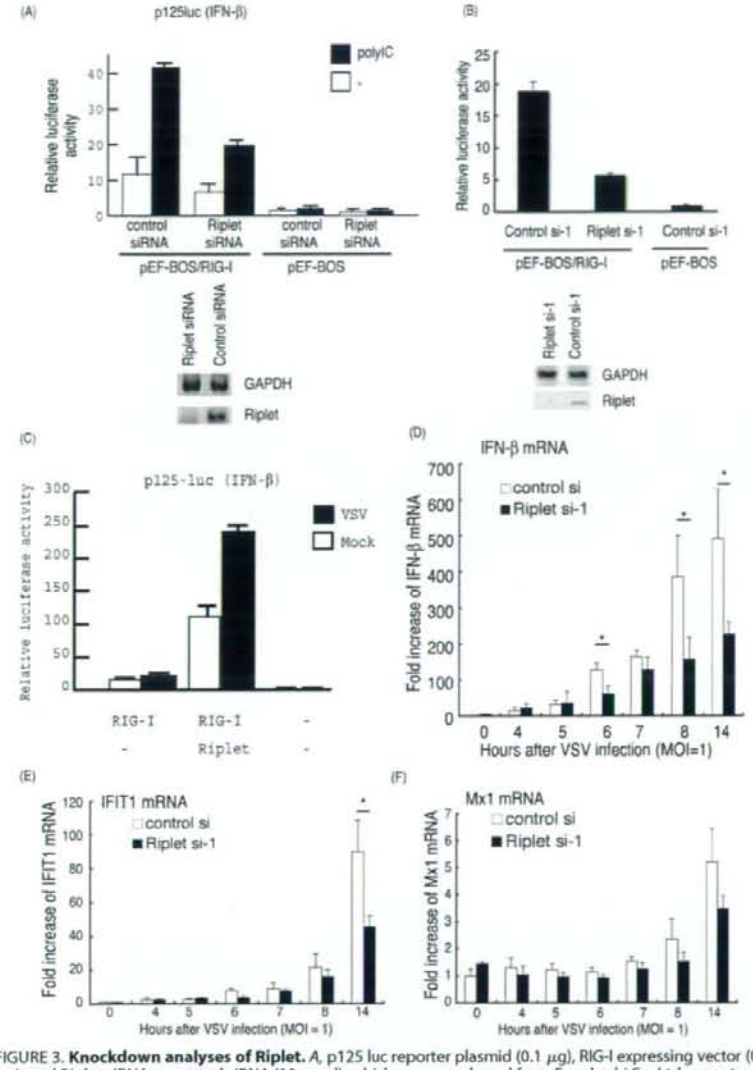

FIGURE 3. **Knockdown analyses of Riplet.** *A*, p125 luc reporter plasmid (0.1 μg), RIG-I expressing vector (0.1 μg), and Riplet siRNA or control siRNA (10 pmol), which were purchased from Funakoshi Co. Ltd., were transfected into HEK293 cells in a 24-well plate with Lipofectamine 2000, and 48 h after transfection, the cells were stimulated with poly(I-C) for 6 h, and the cell lysate was prepared, and luciferase activities were measured. RT-PCR was carried out using total RNA extracted from cells 48 h after transfection. *B*, p125 luc reporter plasmid (0.1 μg), RIG-I expressing vector (0.1 μg), and siRNA, Riplet si-1, or control si-1 (10 pmol), which were purchased from Applied Biosystems, were transfected into HEK293 cells with Lipofectamine 2000. 48 h after transfection, the cells were stimulated with poly(I-C) for 6 h. The cell lysate was prepared, and luciferase activities were measured. RT-PCR was carried out using total RNA extracted from cells 48 h after transfection. *C*, HEK293 cells were transfected with the plasmids expressing RIG-I (0.1 μg) and/or Riplet (0.1 μg) with p125 luc reporter plasmid (0.1 μg) in 24-well plates. After 24 h, the cells were infected with VSV (m.o.i. = 1) for 12 h. The luciferase activities of the cell lysates were measured. Expression of Riplet strongly enhanced IFN-β promoter activation by VSV through RIG-I. *D–F*, siRNA (control si- or Riplet si-1) were transfected into HEK293 cells, and after 48 h, the cells were infected with VSV at m.o.i. = 1. RNA was extracted at the indicated hours, and the quantitative PCR were carried out to detect the expression of IFN-β (*D*), IFIT-1 (*E*), or Mx1 (*F*) mRNA. *, $p < 0.05$. *GAPDH*, glyceraldehyde-3-phosphate dehydrogenase.

IFN-β promoter was only minimally activated by RIG-I in response to VSV (m.o.i. = 1) during the early phase of infection (<12 h), the activity was increased by RIG-I and Riplet (Fig. 3*C*). Riplet was silenced by siRNA and then VSV infected the cells. VSV-derived up-regulation of IFN-β mRNA was started around 6 h post-infection, and Riplet siRNA significantly suppressed the increase of IFN-β mRNA at 6 h (Fig. 3*D*). Because VSV infection is mainly sensed by RIG-I, this is consistent with the notion that Riplet promotes the RIG-I signaling. Other IFN-inducible genes, *IFIT1* and *MX1*, were expressed >8 h post-infection, and their expressions were also suppressed by Riplet siRNA (Fig. 3, *E* and *F*).

Riplet Exerts Protective Activity against Viral Infection—Next we examined the role of Riplet during viral infection. Riplet and/or RIG-I were transiently expressed in the human cells by FuGENE HD reagents, and then the cells were infected with VSV or poliovirus (a positive-stranded RNA virus). The viral titer of the supernatant was determined 24 h post-infection. Under our conditions, expression of RIG-I weakly inhibited VSV propagation. Co-expression of Riplet with RIG-I significantly suppressed VSV replication especially at low m.o.i., whereas Riplet alone did not suppress VSV (Fig. 4, *A* and *B*, *upper panel*). Therefore, a sufficient amount of RIG-I protein is required for Riplet to exert antivirus activity. This requirement of RIG-I is also observed in reporter gene analyses (Fig. 2). Under a similar setting, the antiviral effect of Riplet was marginally observed against poliovirus, which induces IFN-β largely via MDA5 (Fig. 4*B*, *lower panel*). To assess the importance of endogenous Riplet for antivirus effect of human cells, Riplet knockdown cells were infected with viruses. In Riplet knockdown cells, the VSV titer was consistently increased compared with the control ($p < 0.05$) (Fig. 4*C*, *left panel*). In addition, infection of Riplet knockdown cells with poliovirus resulted in only a slight increase in the poliovirus titer compared with the control ($p > 0.05$) (Fig. 4*C*, *right panel*). Because poliovirus is mainly recognized by MDA5 but not RIG-I, this marginal effect of Riplet on poliovirus infection was within expectation (3, 28).

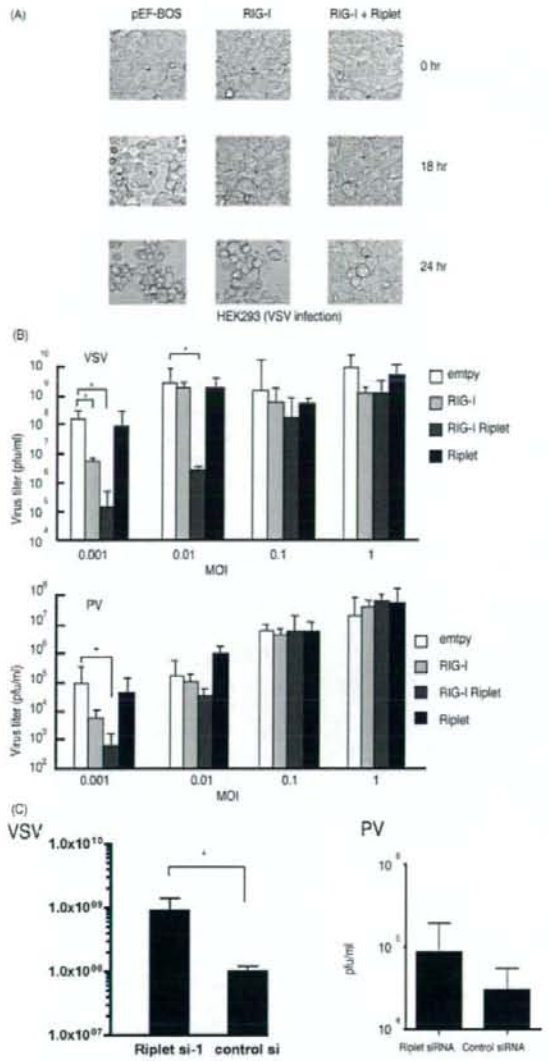

FIGURE 4. **Suppression of RNA viruses by Riplet.** *A*, HEK293 cells were transfected with RIG-I (0.1 μg) and/or Riplet (0.1 μg) expressing vectors. The total amount of transfected DNA (0.5 μg/well) in each well was kept constant by adding empty vector (pEF-BOS). 24 h after transfection, the cells were infected with VSV at m.o.i. = 0.1, and after 0, 18, or 24 h, CPE was observed by microscope. *B*, RIG-I (0.1 μg) and/or Riplet (0.1 μg) expressing plasmids were transfected to HEK293 cells in 24-well plates and incubated for 24 h. The total amount of transfected DNA (0.5 μg/well) in each well was kept constant by adding empty vector (pEF-BOS). The cells were infected with VSV (*upper panel*) or poliovirus (*PV*) (*lower panel*) at the indicated m.o.i. The viral titers in the culture media were measured 24 h after infection by plaque assay. *Error bars* represent standard deviation ($n = 3$). *, $p < 0.05$. *C*, control or Riplet knockdown HEK293 cells were infected with VSV (*left panel*) or poliovirus (*right panel*) at m.o.i. = 0.1. The viral titers in the culture media were measured 26 h after infection by plaque assays. Knockdown of Riplet induced higher VSV titers compared with control ($p < 0.05$), but the increase observed in poliovirus-infected Riplet knockdown cells was not significant ($p > 0.05$).

Riplet and Riplet-DN Bind the Helicase and RD Regions of RIG-I—Yeast two-hybrid analysis showed that a C-terminal region of Riplet bound to the C-terminal region of RIG-I. This cytoplasmic interaction between Riplet and RIG-I was confirmed by confocal microscopy in HeLa cells (supplemental Fig. S2). To further confirm the physical binding of Riplet to RIG-I in human cells, we carried out immunoprecipitation analyses. Full-length Riplet was co-immunoprecipitated with RIG-I (Fig. 5*B*), indicating that Riplet binds directly to RIG-I in human cells.

To determine the region responsible for the RIG-I-Riplet interaction, we constructed a RIG-I and Riplet deletion series as shown in Fig. 5*A*. Riplet-DN also bound to RIG-I (Fig. 5, *B* and *C*), indicating that the RING finger domain is dispensable for the RIG-I-Riplet interaction. This is consistent with the notion that the RING finger domain in ubiquitin ligase proteins is required for their interactions with ubiquitin-conjugating enzymes (29). Unlike TRIM25, Riplet and Riplet-DN failed to co-precipitate the two CARD domains of RIG-I (dRIG-I) (Fig. 5*D*). However, co-precipitation of the RIG-IC or RIG-RD fragments was observed (Fig. 5, *E* and *F*). RD-deleted RIG-I (RIG-I dRD) weakly associated with Riplet (Fig. 5*G*). Taken together, Riplet preferentially binds the RD and also weakly associates with the helicase region of RIG-I with its C terminus. Reporter gene analyses show that Riplet-DN only weakly suppresses RIG-I signaling and barely suppresses dRIG-I, which contains neither helicase nor RD region. Therefore, the physical interaction is correlated with the results of reporter activity.

Riplet Promotes Ubiquitination of RIG-I—Because Riplet shares 60% sequence similarity with TRIM25, we hypothesized that Riplet ubiquitinates RIG-I and that this modification leads to activation of RIG-I signaling. To test this hypothesis, we examined RIG-I ubiquitination. As expected, ubiquitination of RIG-I was increased by co-expression of Riplet under two different conditions (Fig. 6, *A* and *B*). The quantity of RIG-I ubiquitination was significantly high in the presence of Riplet (Fig. 6*C*). RIG-I ubiquitination was suppressed if Riplet was replaced with Riplet-DN (Fig. 6*D* and supplemental Fig. S4*C*). However, unlike TRIM25, Riplet binds to the C-terminal region of RIG-I. Therefore, we examined whether Riplet ubiquitinates the C-terminal region. We found that ubiquitination of RIG-IC was enhanced by Riplet expression (Fig. 6*E*). Both RIG-I dRD and RIG-I RD were also ubiquitinated by expression of Riplet (Fig. 6*F*; supplemental Fig. S4*A* and S5), suggesting that Riplet promotes ubiquitination of the helicase and RD domains of RIG-I in a manner distinct from TRIM25.

Ubiquitin is polymerized through its lysine residue. Lys-63-linked polyubiquitination is frequently observed in signal transduction pathways (30). In contrast, Lys-48-linked polyubiquitination usually leads to the degradation of protein through the proteasome. Indeed, TRIM25-mediated Lys-63-linked polyubiquitination activates the CARD-like region of RIG-I, and RNF125-mediated Lys-48-linked polyubiquitination leads to the degradation of RIG-I (23, 25). We used K48R or K63R mutated ubiquitin and found that K48R was incorporated normally into RIG-IC, whereas polyubiquitination was decreased by K63R (supplemental Fig. S4*B*). K63R mutation abolished RIG-I RD polyubiquitination by Riplet (Fig. 6*F*). These data

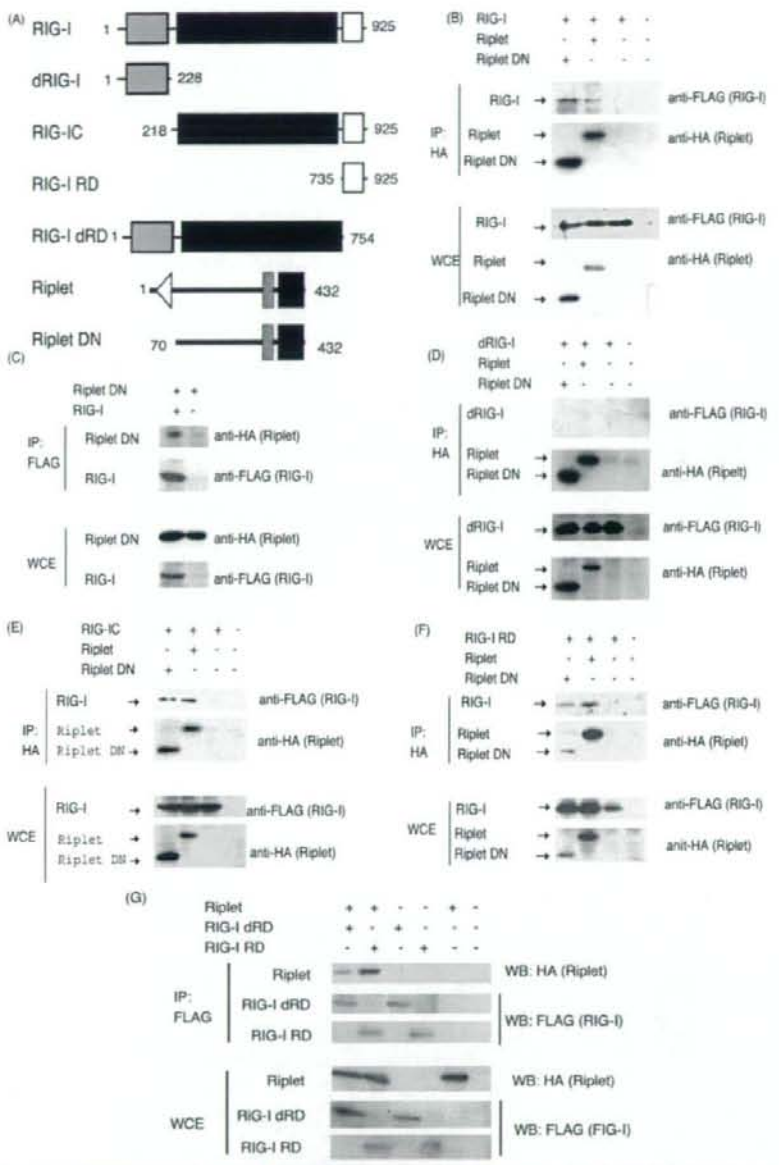

FIGURE 5. **Physical interaction of Riplet with RIG-I.** *A*, schematic representation of RIG-I or Riplet fragments used for immunoprecipitation analyses. *B*, HA-tagged Riplet (0.4 μg) or Riplet-DN (0.4 μg) were transfected into HEK293FT cells in a 6-well plate with FLAG-tagged RIG-I (0.4 μg). HA-tagged Riplet or Riplet-DN were immunoprecipitated (*IP*) with anti-HA antibodies, and samples were analyzed by Western blotting (*WB*) using an anti-FLAG or anti-HA antibody. The total amount of transfected DNA (2 μg/well) was kept constant by adding empty vector (pEF-BOS). *C*, HA-tagged Riplet-DN (0.4 μg) and FLAG-tagged RIG-I (0.4 μg) were transfected into HEK293FT cells in a 6-well plate. RIG-I was immunoprecipitated with anti-FLAG antibody, and samples were analyzed by Western blotting using an anti-FLAG or -HA antibody. The total amount of transfected DNA (2 μg/well) was kept constant by adding empty vector (pEF-BOS). *D–F*, interaction of HA-tagged Riplet or Riplet-DN with FLAG-tagged dRIG-I (*D*), RIG-IC (*E*), or RIG-I RD (*F*) was examined using immunoprecipitation assays. The proteins were expressed in HEK293FT cells, and HA-tagged Riplet was immunoprecipitated with anti-HA antibody, and samples were analyzed by Western blotting using an anti-FLAG or -HA antibody. *G*, FLAG-tagged RIG-I RD (0.4 μg) or RIG-I dRD (0.4 μg) was transfected with HA-tagged Riplet (0.4 μg) into HEK293 FT cells in a 6-well plate, and 24 h after transfection, immunoprecipitation was performed with anti-FLAG antibody and analyzed by Western blotting. The total amount of transfected DNA (2 μg/well) was kept constant by adding empty vector (pEF-BOS). *WCE*, whole cell extract.

indicates that Riplet mediates Lys-63-linked polyubiquitination of the RIG-I C-terminal helicase and RD region. Because Riplet-DN reduced the RIG-I-mediated signaling, we examined whether Riplet-DN reduced the RIG-I ubiquitination. As expected, Riplet-DN reduced RIG-I ubiquitination (Fig. 6*D* and supplemental Fig. S4*C*). These ubiquitination assay data are consistent with the notion that Riplet-mediated Lys-63-linked polyubiquitination of RIG-I is required for full activation of RIG-I signaling.

We tried to determine the ubiquitination sites of RIG-I using Lys-to-Ala (KA)-converting mutants. RIG-I has 25 Lys residues in its C-terminal region. These Lys residues of RIG-I were in turn mutated to Ala, and the degree of ubiquitination and IFN-β-inducing activity were determined with each mutant. RIG-I-mediated IFN-β promoter activation was normally augmented by co-expression of Riplet and 3KA RIG-I. Co-expression of Riplet and 5KA, however, and the ubiquitination level of RIG-I and IFN-β-inducing activity were simultaneously decreased (Fig. 7, *A* and *C*). Riplet-dependent augmentation of IFN-β promoter activation was largely suppressed when RIG-I was replaced with 5KA RIG-I (Fig. 7*B*). Therefore, Lys-849 and Lys-851 of RIG-I were crucial for RIG-I ubiquitination by Riplet. The results confirmed the importance of ubiquitination of specific Lys residues in the C-terminal region of RIG-I and for RIG-I-mediated IFN-β induction.

DISCUSSION

RIG-I plays a central role in the recognition of cytoplasmic viral RNA and is regulated by modification by small modifier ubiquitin or ubiquitin-like protein, ISG15. TRIM25 mediates Lys-63-linked polyubiquitination, which is essential for RIG-I activation (23), and RNF125 mediates Lys-48-linked polyubiquitination (25). RIG-I also harbors ISG15 modification, although the role of ISG15 modification *in vivo* remains to be deter-

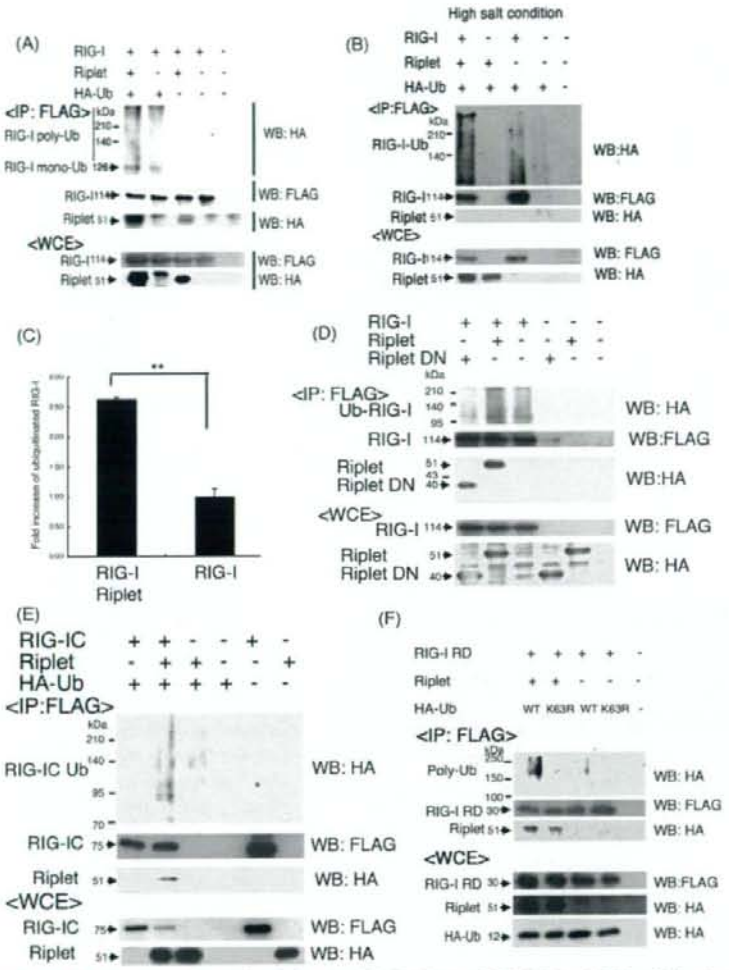

FIGURE 6. **Ubiquitination of RIG-I by Riplet.** *A* and *B*, FLAG-tagged RIG-I (0.4 μg), Riplet (0.4 μg), and HA-tagged ubiquitin (0.4 μg) expressing vectors were transfected into HEK293FT cells in 6-well plates. The total amount of transfected DNA (2 μg/well) was kept constant by adding empty vector (pEF-BOS). FLAG-tagged RIG-I was immunoprecipitated (*IP*) using an anti-FLAG antibody, and washed with the buffer containing 150 mM NaCl (*A*) or 1 M NaCl (*B*). The immunoprecipitates were separated with 8% acrylamide gel and analyzed by Western blotting (*WB*) using antibodies against HA tag (ubiquitin) or FLAG (RIG-I). Riplet was co-immunoprecipitated with FLAG-tagged RIG-I in *A* but could not co-immunoprecipitate in *B* because of high salt condition. Expression of Riplet enhanced the ubiquitination of RIG-I. Different gel conditions were employed in *A* and *B*. *C*, ubiquitinated RIG-I was quantitated with NIH image software. **, $p < 0.01$. *D*, FLAG-tagged RIG-I (0.4 μg) was transfected into HEK293 FT cells in a 6-well plate with HA-tagged Riplet (0.4 μg) or Riplet-DN (0.4 μg) and HA-tagged ubiquitin, and immunoprecipitation was carried out with anti-FLAG antibody. The total amount of transfected DNA (2 μg/well) was kept constant by adding empty vector (pEF-BOS). The samples were analyzed with 10% acrylamide gel to clearly separate Riplet from Riplet-DN and stained by Western blotting. *E*, ubiquitination of RIG-IC was also promoted by Riplet expression. HEK293FT cells were transfected with the plasmids encoding RIG-IC (0.4 μg), Riplet (0.4 μg), and/or HA-tagged ubiquitin (0.4 μg) in a 6-well plate, and 24 h after transfection, cell lysates were prepared. The total amount of transfected DNA (2 μg/well) was kept constant by adding empty vector (pEF-BOS). FLAG-tagged RIG-ICs were immunoprecipitated with anti-FLAG antibodies, and the proteins were analyzed by Western blotting. *F*, Ub-K63R are HA-tagged ubiquitin in which the lysine 3 residues were substituted with arginine. The HA-tagged Ub-K63 expressing vectors (1.2 μg), FLAG-tagged RIG-IC (0.4 μg), and/or Riplet (0.4 μg) were transfected into HEK293FT cells in 6-well plates and analyzed as shown in *A–D*. The total amount of transfected DNA (2 μg/well) was kept constant by adding empty vector (pEF-BOS). Ub-K63R was not incorporated into polyubiquitin chain of RIG-I RD. *WCE*, whole cell extract.

mined (21, 22, 31). Although Riplet and TRIM25 share 60% sequence similarity, the ubiquitination of RIG-I by Riplet is distinct from that by TRIM25; Riplet ubiquitinates the C-terminal region of RIG-I, whereas TRIM25 ubiquitinates its CARD-like region. These findings are also supported by the fact that neither Riplet nor Riplet-DN promoted or inhibited the activation of the IFN-β promoter by expression of the RIG-I CARD-like region (data not shown). It has been reported that ubiquitination of the CARD-like region of RIG-I by TRIM25 is critical for RIG-I-IPS-1 signaling (23). However, how this CARD ubiquitination is essential for activation of IPS-1 by RIG-I remains undetermined. Here we emphasize the importance of RIG-I C-terminal ubiquitination for IFN-β induction and the antiviral response. Because the C-terminal RD region inhibits the IFN inducing activity of the CARD-like region of RIG-I, it is reasonable that RIG-I C-terminal ubiquitination by Riplet inhibits the conversion from the active to inactive form of RIG-I protein after binding to viral RNA. This initial stabilization of RIG-I via ubiquitination by Riplet would provide a sufficient structure for RIG-I to maintain the accessibility to TRIM25 and facilitate TRIM25-mediated ubiquitination of the CARD-like region of RIG-I, which may lead to potential activation of IPS-1.

RIG-I is an IFN-inducible RNA helicase that is expressed at extremely low levels in resting cells (6). Initial penetration of viruses allows generation of 5′-triphosphate RNA and/or double strand RNA followed by induction of IFN-β production. This early response to viral infections triggers up-regulation of RIG-I/MDA5 and TLR3, leading to robust IFN-β production (3, 32, 33). We favor the interpretation of our present findings that during the early stages of viral infection with trace amounts of RIG-I and viral RNAs, Riplet helps host cells rearrange RIG-I conformation to activate IPS-1. This issue will need further proof because it is difficult to

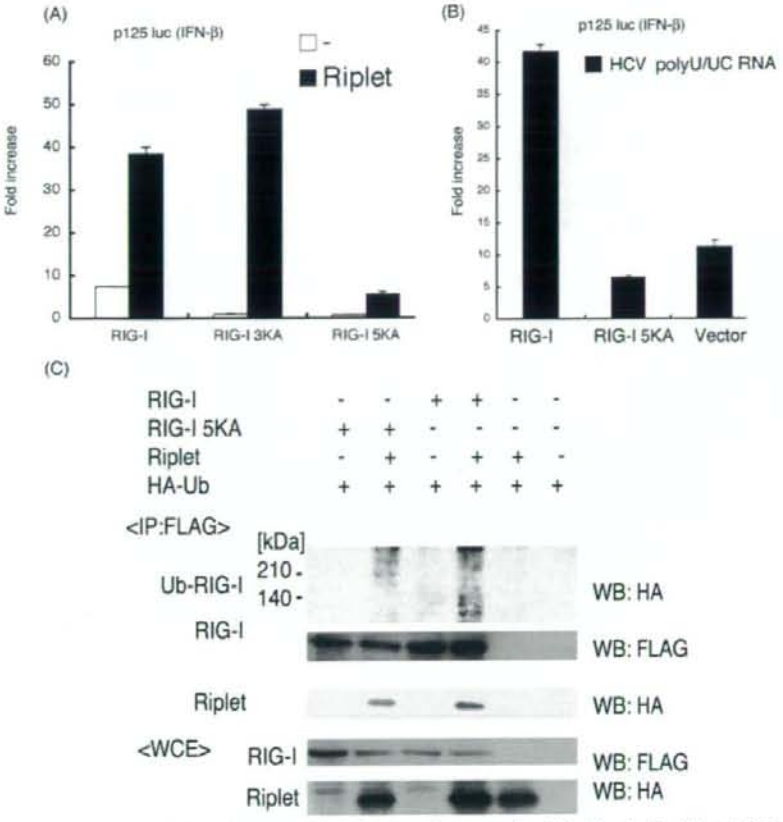

FIGURE 7. **The C-terminal two lysine residues of RIG-I are important for ubiquitination by Riplet.** *A*, RIG-I C-terminal lysine residues were substituted with alanine. RIG-I 3KA mutant protein harbors the triple mutations, K888A, K907A, and K909A. The five lysine residues, Lys-849, Lys-851, Lys-888, Lys-907, and Lys-909, were replaced with alanine in RIG-I 5KA mutant. The plasmid carrying wild-type (100 ng/well), RIG-I 3KA (100 ng/well), RIG-I 5KA (100 ng), or Riplet (100 ng) were transfected into HEK293 cells in a 24-well plate together with p125 luc reporter plasmid (100 ng/well). The amount of transfected DNA was kept constant by adding empty vector. After 24 h, the luciferase activities were measured. *B*, wild-type RIG-I (100 ng), RIG-I 5KA mutant (100 ng), or empty vector (100 ng) was transfected into HEK293 cells in a 24-well plate together with p125 luc reporter plasmids and HCV 3′-untranslated region poly(U/UC) RNA (25 ng), which is synthesized in *in vitro* transcription by T7 RNA polymerase. The amount of transfected DNA was kept constant by adding empty vector. 24 h after transfection, luciferase activities were measured. RIG-I 5KA mutant hardly responded to poly(U/UC) RNA. *C*, to observe the ubiquitinated RIG-I more clearly, we used 800 ng/well of Riplet and HA-Ub expression vector for the following transfection. HEK293FT cells in a 6-well plate were transfected with the plasmids encoding RIG-I (400 ng/well), RIG-I 5KA (400 ng/well), Riplet (800 ng/well), and/or HA-Ub (800 ng/well). The total amount of DNA was kept constant by adding the empty vector. 24 h after the transfection, the cell lysates were prepared, and the immunoprecipitation was carried out using anti-FLAG antibodies. The immunoprecipitates were analyzed by Western blotting with anti-HA or FLAG antibodies.

visualize RNRs and viral RNAs in the early infection stage and to understand the mechanisms that allow viruses to uncoat into naked viral RNA and to replicate.

We have provided several lines of evidence indicating that Riplet complements RIG-I-mediated IFN-β induction upon viral infection by both Riplet siRNA and overexpression analyses. The C-terminal lysines (849 and 851) of RIG-I are critical for Riplet-mediated RIG-I ubiquitination. However, our data indicate that Riplet alone was unable to induce IFN-β production and essentially required RIG-I to confer IFN-β induction. Furthermore, Riplet is not ubiquitously distributed over the organs tested. Ubiquitination of RIG-I induced by poly(I-C) or viruses was accelerated in cells pre-transfected with Riplet. Hence, Riplet works case-sensitive to up-regulate RIG-I antiviral activity predominantly in some organs. The physiological meaning of this response will be clarified by knock-out study.

Unexpectedly, the siRNA experiments were not robust with regard to VSV replication. Possible explanations for this are as follows: 1) the degree of gene silencing is not so profound that the proteins remain in the cells; 2) there are a number of virus-mediated IFN-inducing pathways capable of compensating each other, so that disruption of one factor does not cause a profound effect on VSV replication. Furthermore, in VSV-infected Riplet-knockdown cells, IFN-β levels were reduced even at m.o.i. = 1 (Fig. 3*D*), and accordingly, virus susceptibility was increased at m.o.i. = 0.1 (Fig. 4*C*), whereas in Riplet-overexpressing cells, antiviral activity was observed only at low m.o.i. (Fig. 4*B*). We used different transfection reagents and cell conditions in the knockdown and overexpression experiments to obtain high transfection efficiency in each. These conditional differences in knockdown and overexpression analyses might cause part of the discrepancy between the two results on Riplet antiviral activity. Another possibility to explain the apparent inconsistencies between overexpression and knockdown analyses is that high amounts of Riplet efficiently activate the RIG-I signaling, but low amounts are insufficient for RIG-I activation in high m.o.i.-infecting human cells. High amounts of Riplet with overexpressed RIG-I would confer the ability on cells to respond to very low amounts of VSV as observed in the low m.o.i. experiments. Again, *riplet* knock-out mice would reveal whether it is absolutely required for potential RIG-I activation.

How viral RNAs select RIG-I rather than dicers or the translation machinery is also unknown. During natural infection it is likely that the number of the initial invading virions would be at most several copies/cell. Uncoated viral RNA may assemble a complex consisting of viral and host molecules required for replication. We assume that cells are equipped with various